STRUCTURE OF GALAXIES

Lecture 9. Elliptical galaxies, Faber-Jackson relation, Fundamental Plane, triaxiality.

a. Surface photometry.

Elliptical galaxies usually conform to the $R^{1/4}$-law and look smooth and regular.

NGC 3379 has been used as a prototype and standard for surface photometry*.

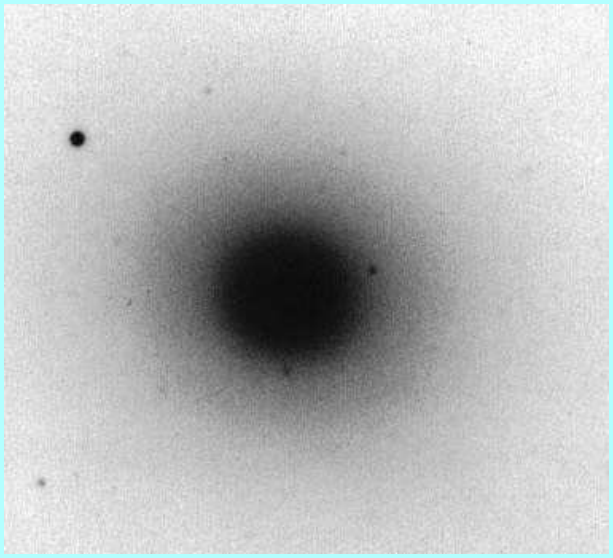

*de Vaucouleurs & Capaccioli, Ap.J.Suppl. 40, 699 (1979)

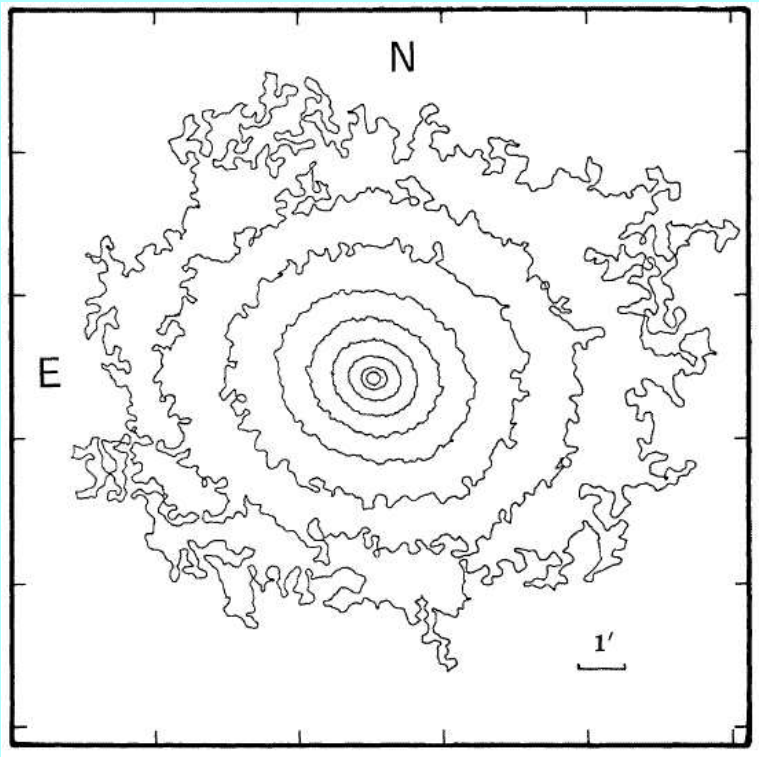
N
E
1′

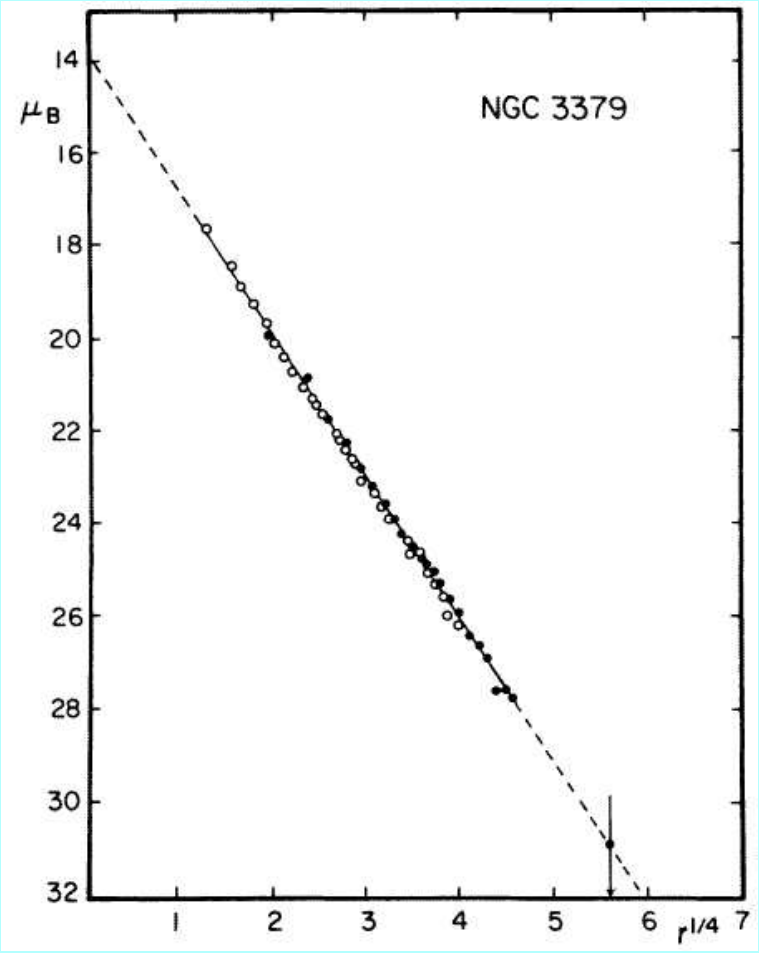
NGC 3379
μ_B
14
16
18
20
22
24
26
28
30
32
1
2
3
4
5
6
7
$r^{1/4}$

Detailed study shows that the isophotal structure of ellipticals is usually much more complicated.

In particular there are isophote twists and deviations from ellipticity.

The latter are described by parameters $a(i)$. These describe the deviations from pure ellipses in multiplicity i*. These are derived from Fourier analysis of the isophote shapes relative to the best fitting ellipse.

By definition (because of the ellipse fit) $a(i) = 0$ for $i = 0, 1, 2$.

The most interesting is $a(4)$, which is negative for "boxy" isophotes and positive for "disky" isophotes.

*Bender, Döbereiner & Möllenhoff, A.&A.Suppl. 74, 385 (1988)

Here are some examples of non-zero parameters $a(4)$.

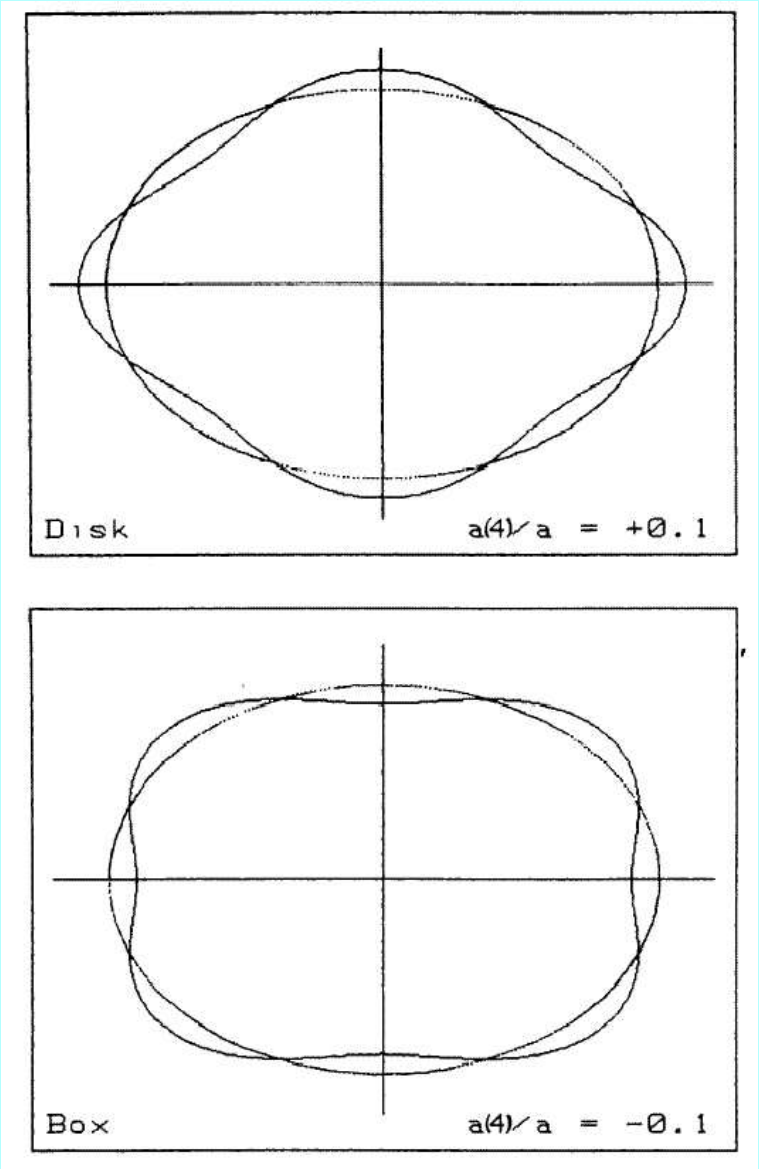

We will now look at fits in a boxy and in a disky galaxy.

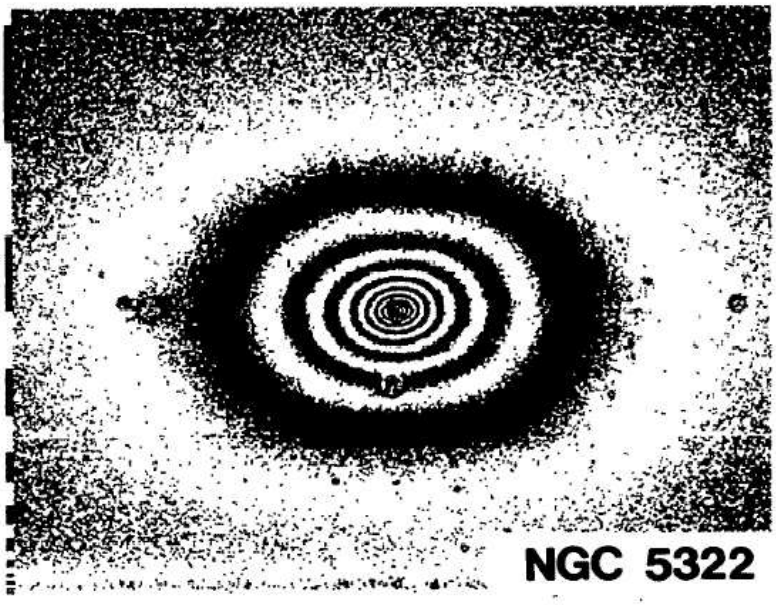

FIGURE 7. — R-image of NGC 5322, an elliptical galaxy with box-shaped isophotes $(a(4)/a \sim -0.01)$.

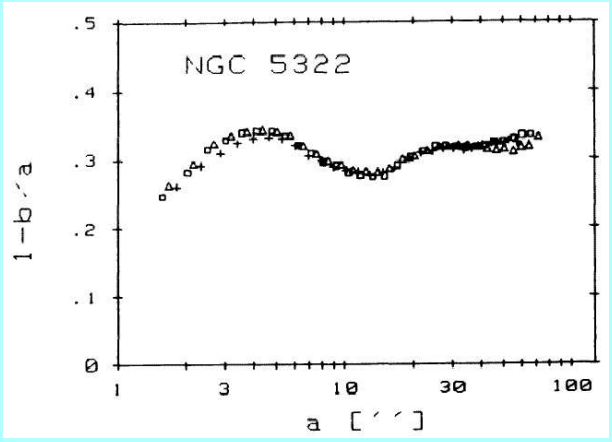

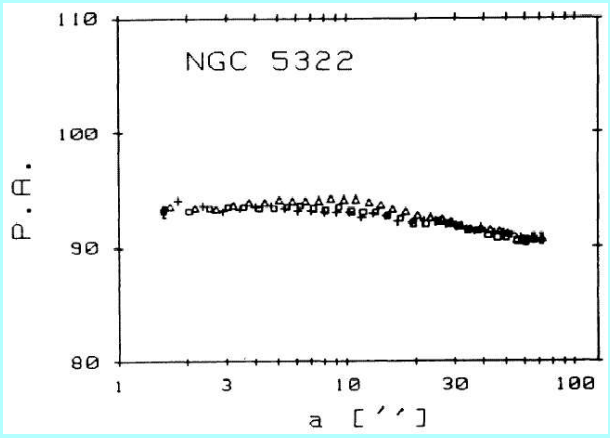

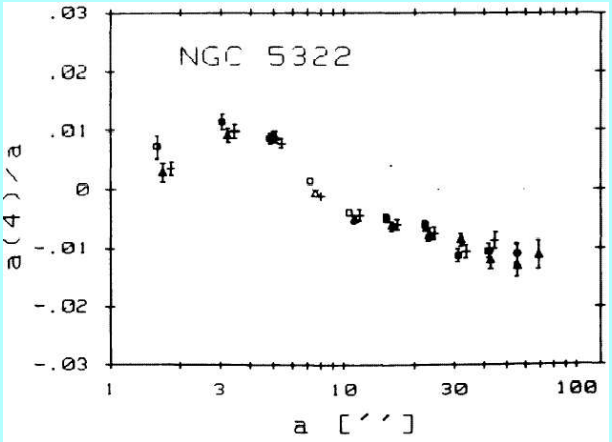

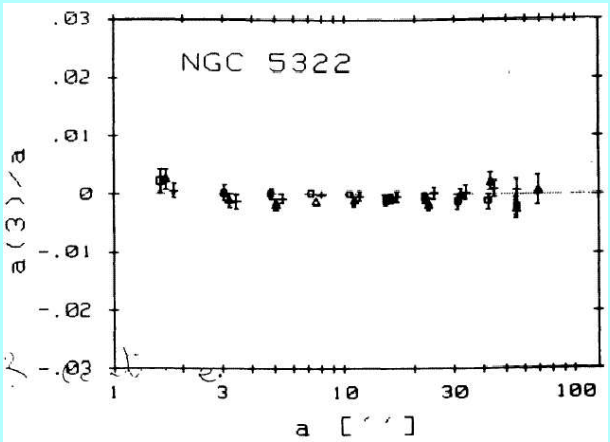

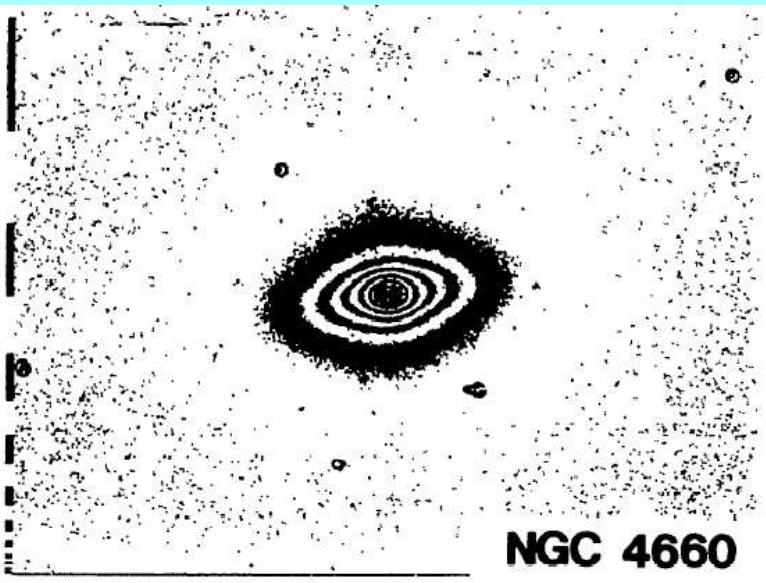

FIGURE 6. — R-image of NGC 4660, an elliptical galaxy with a disk-component in the isophotes $(a(4)/a \sim +0.03)$.

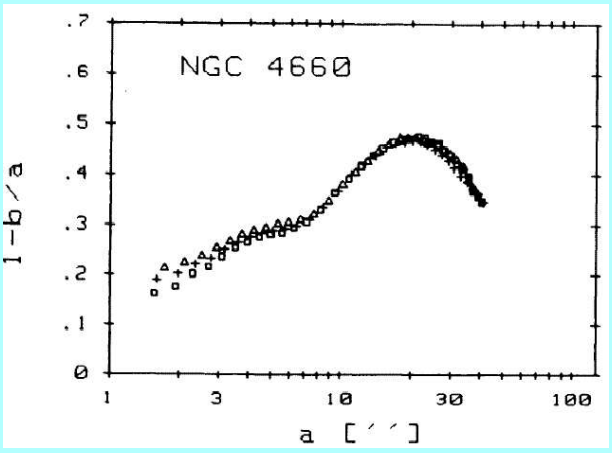

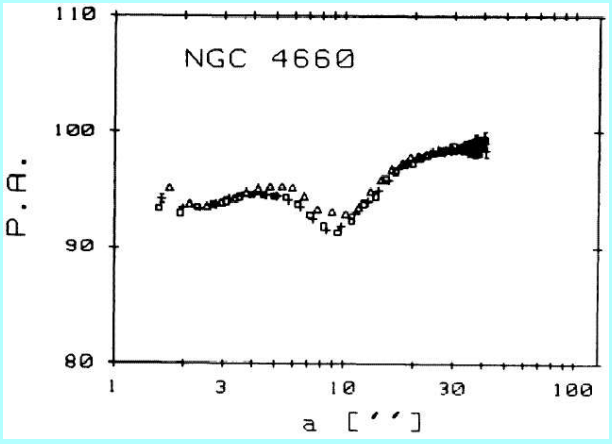

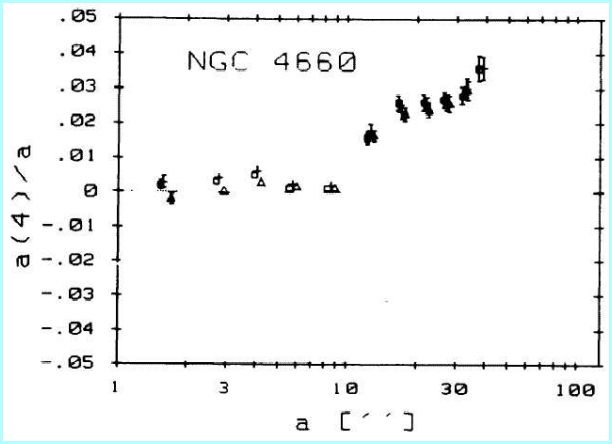

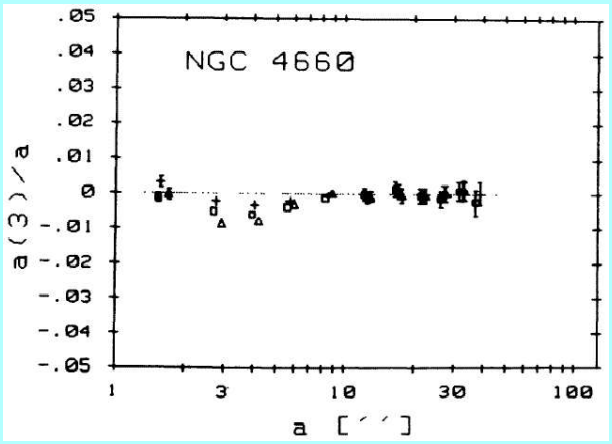

The global $a(4)$ parameter for a sample of galaxies does not correlate with effective radius or integrated luminosity*.

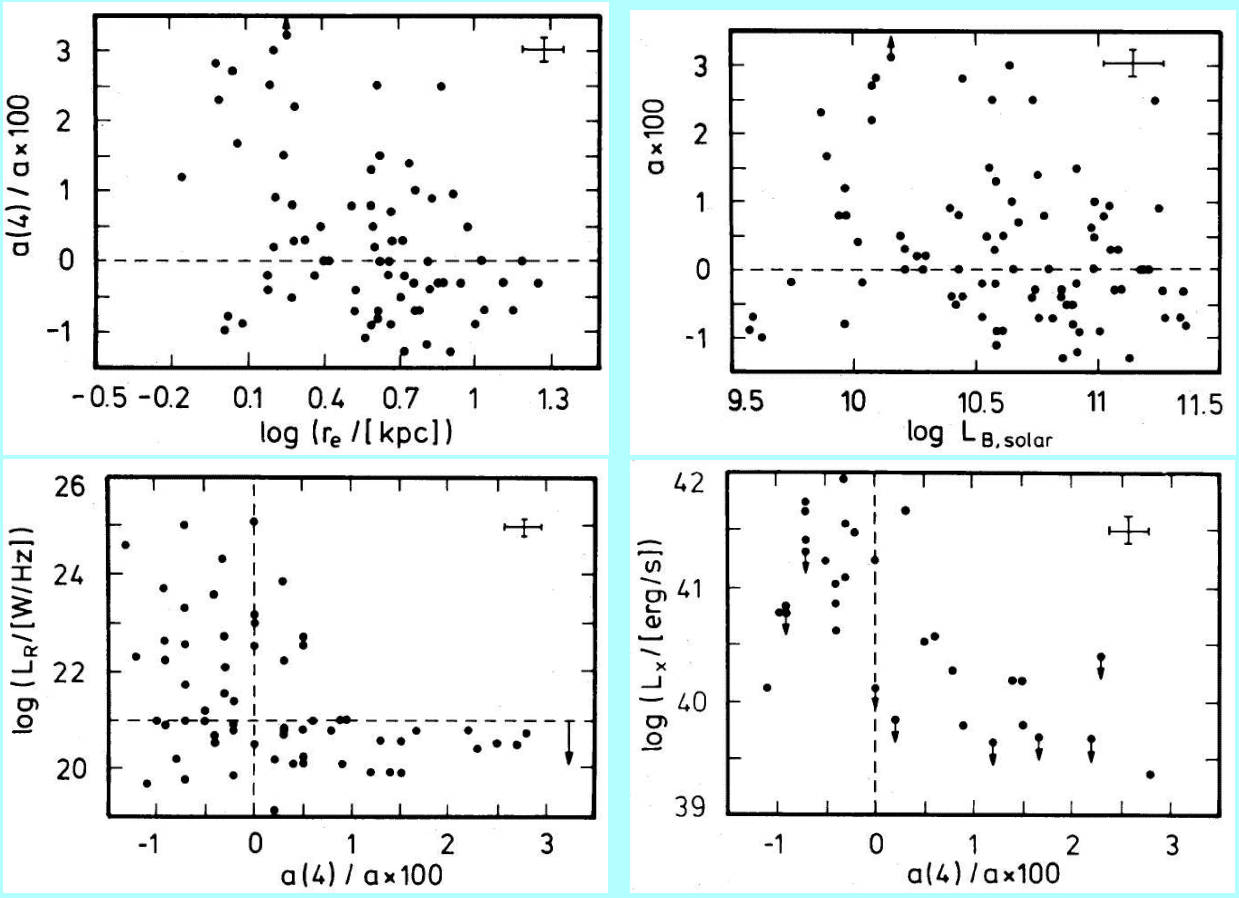

However, galaxies with strong radio emission or X-ray halo's are almost always boxy.

It has been suggested that "boxyness" results from interactions.

*Bender, Surma, Döbereiner, Möllenhoff & Madejsky, A.&A. 217, 35 (1989)

There is a well-defined color – magnitude relation for early-type galaxies*.

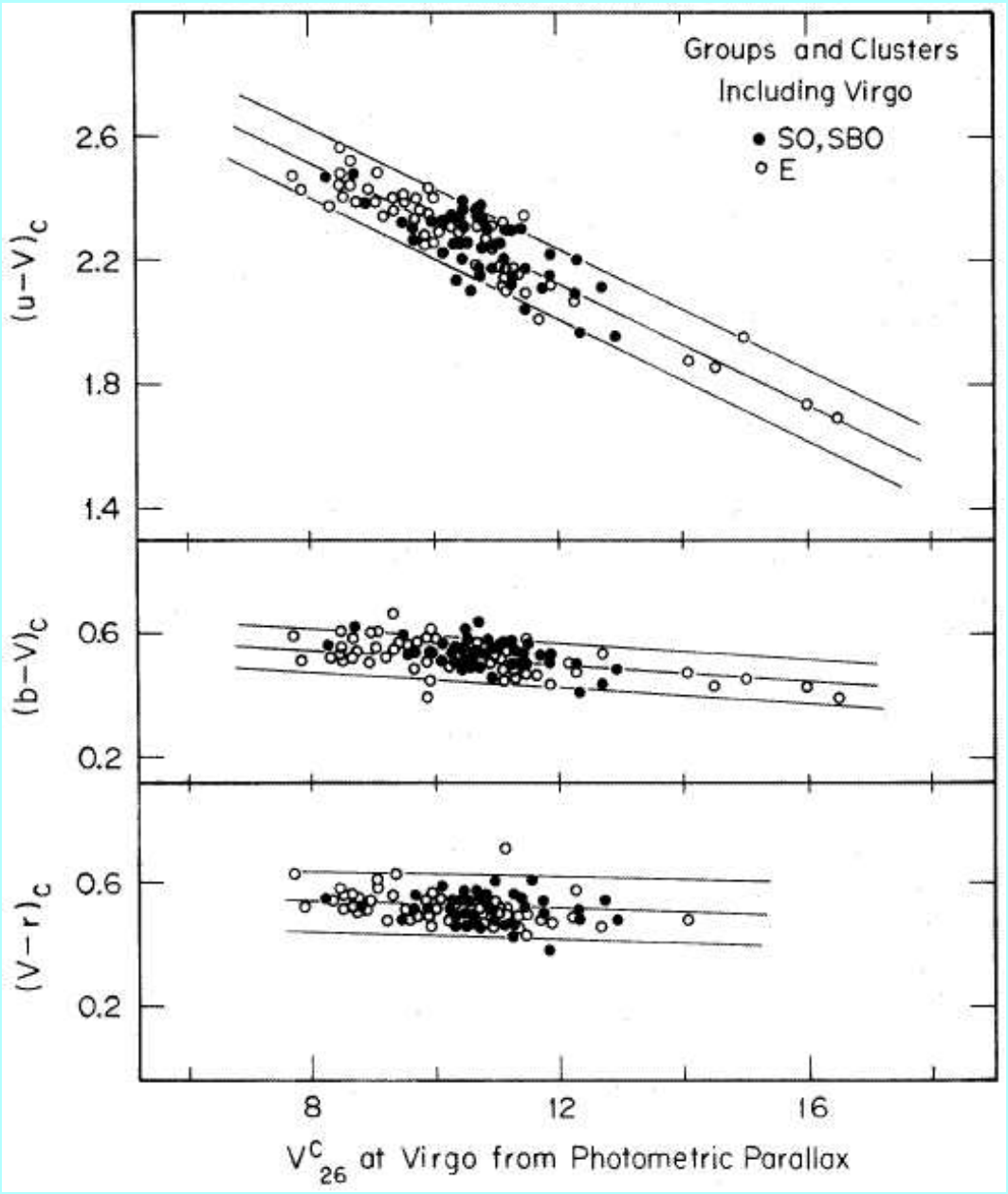

*Sandage, Ap.J. 176, 21 (1972); Visvanathan & Sandage, Ap.J. 216, 214 (1977); Sandage & Visvanathan, Ap.J. 223, 707 and 225, 742 (1978)

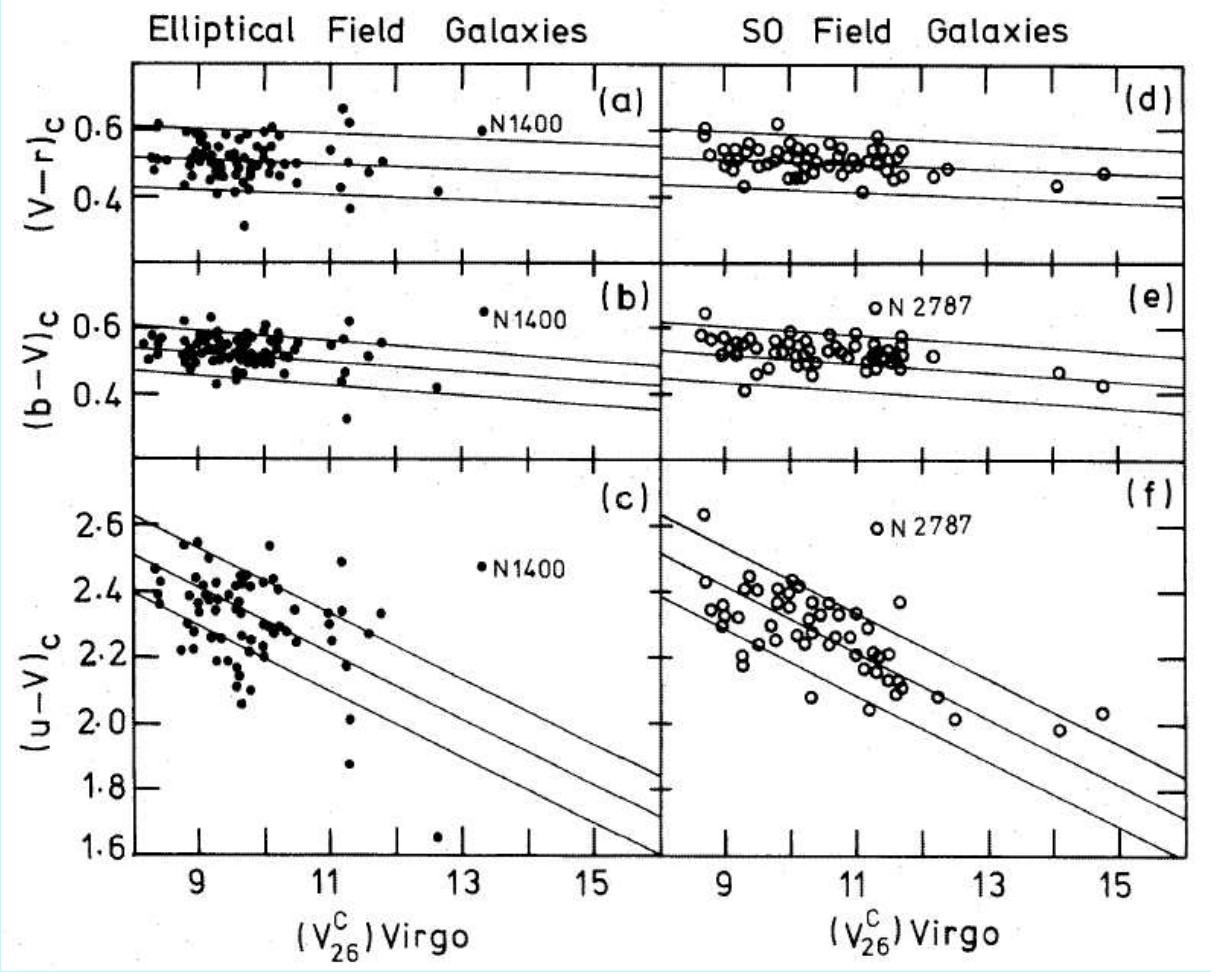

The relation is the same in clusters and in the field.

It is actually one between metallicity and mass (or escape velocity).

The luminosity function of galaxies is fitted with the Schechter-function*

$$\phi(L)dL \propto (L/L^\star)^\alpha \text{ exp } (-L/L^\star)d(L/L^\star)$$

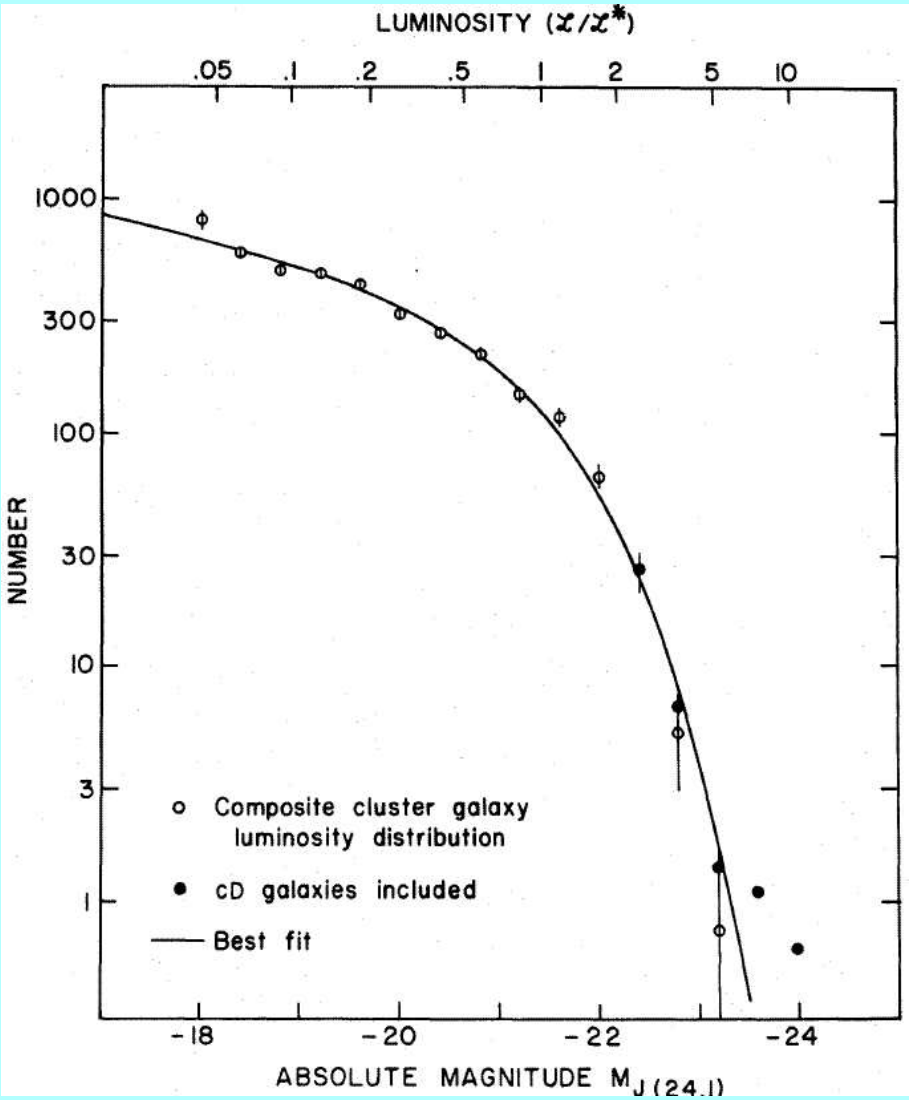

The best fits have $\alpha \sim 1.2$ and $L^\star$ corresponding to $M_B^\star \sim -20.6$.

*Ap.J. 203, 297 (1976)

In the outer parts faint "shells and ripples" are seen, such as in NGC 1316 = Fornax A*.

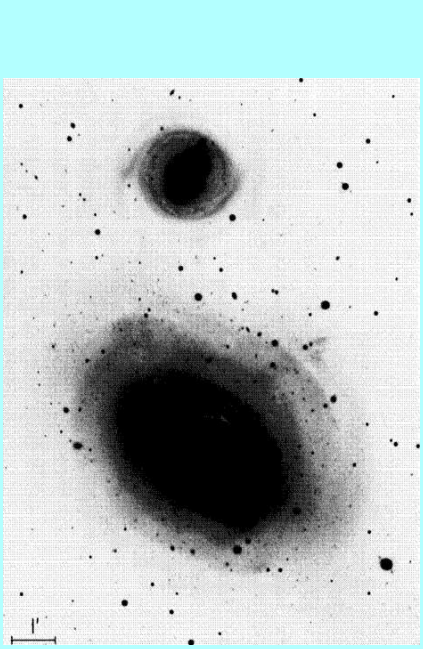

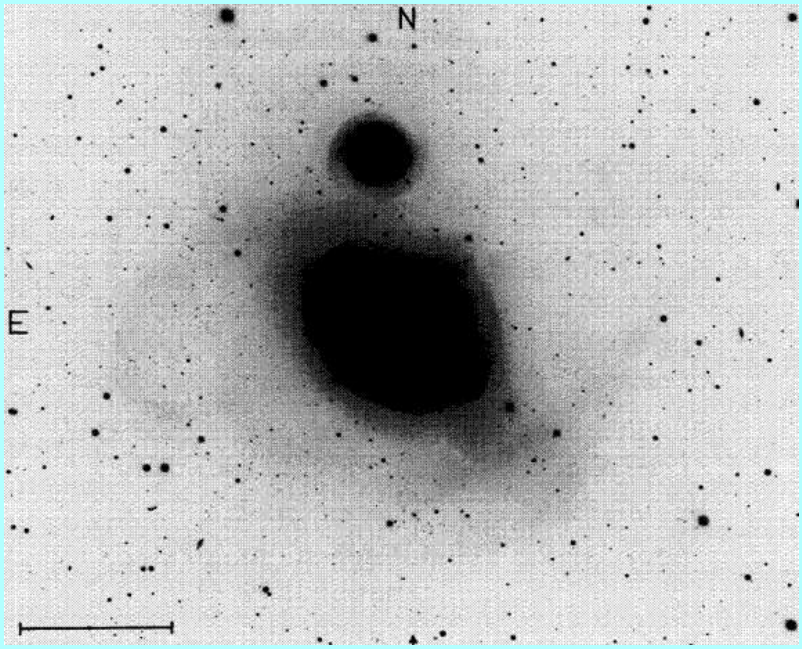

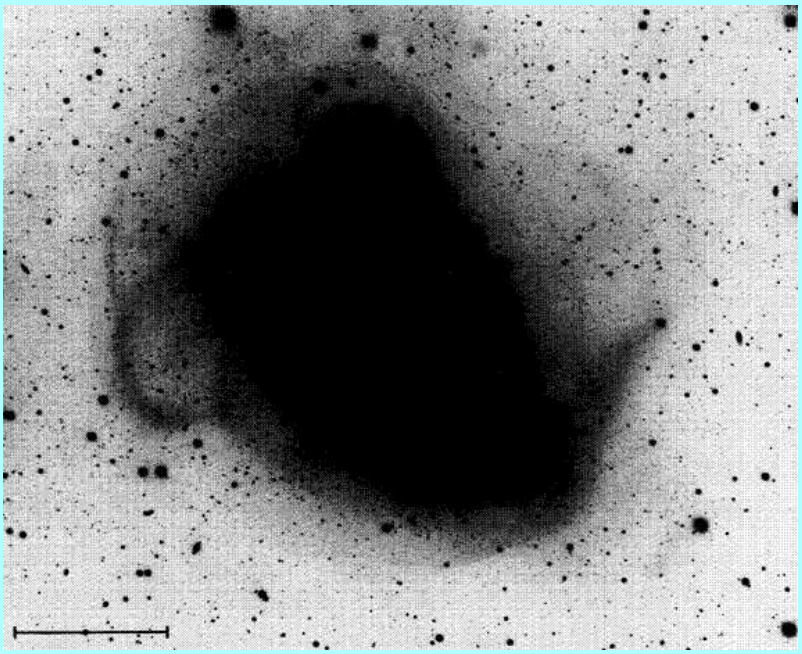

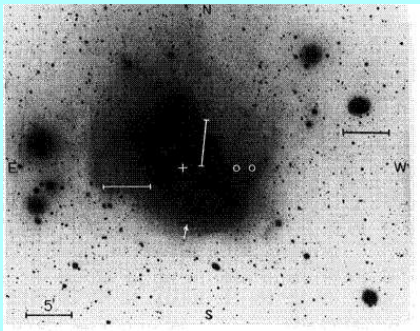

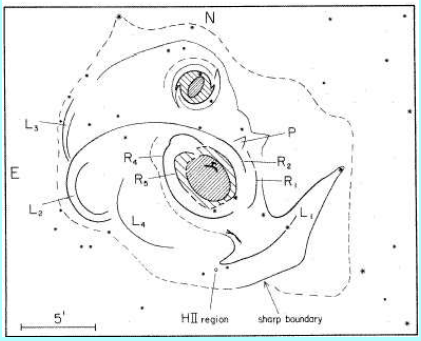

*Schweizer, Ap.J. 237, 303 (1980)

Numerical experiments* show that these can be the result of a collission with a disk galaxy.

In the figure below we see how the disk evolves in the potential of a 100 times more massive elliptical galaxy in a typical encounter.

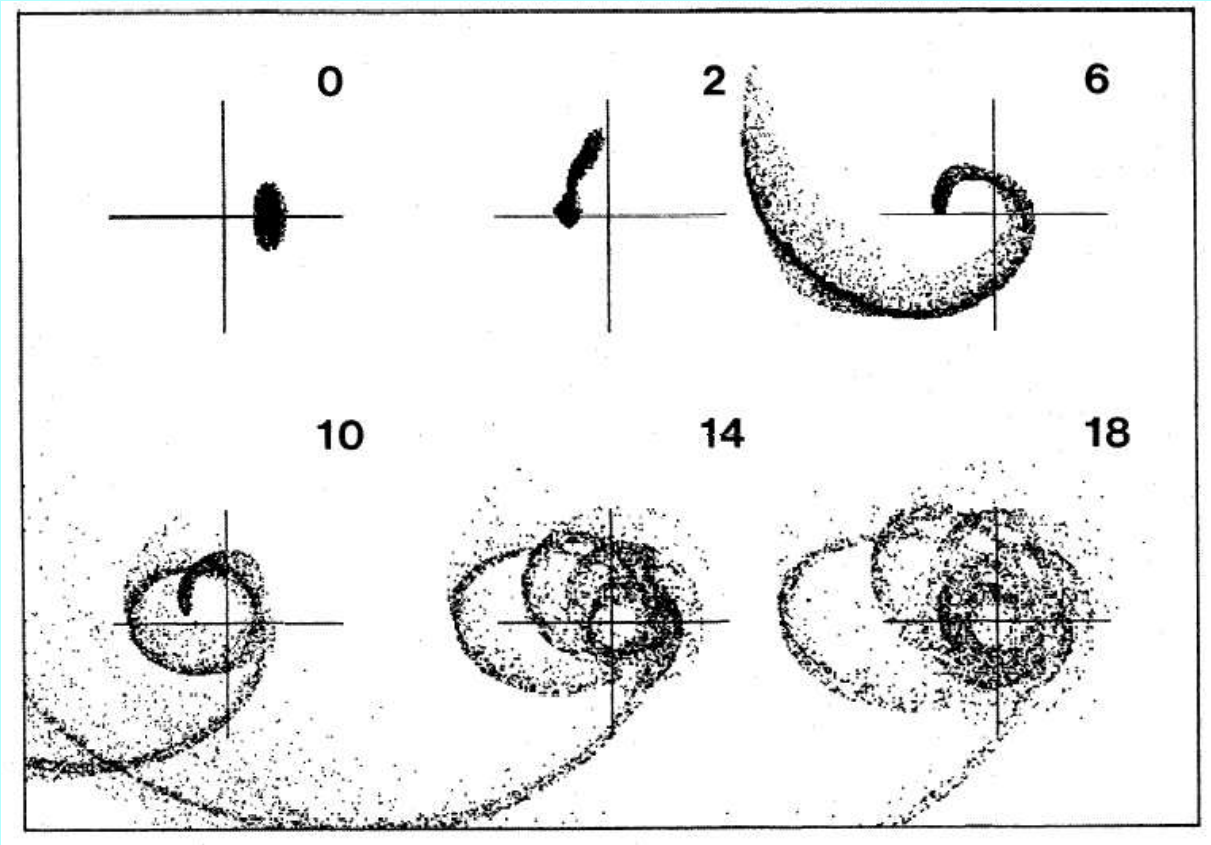

The unit of time is the circular period at a characteristic radius in the potential.

*Quinn, Ap.J. 279, 596 (1984)

b. Kinematics.

The isothermal sphere has at large R

$$\rho(R) = \frac{\langle V^2 \rangle}{2\pi G} R^{-2}$$

The core radius is

$$r_\circ = \left(\frac{4\pi G \rho_\circ}{9\langle V^2 \rangle} \right)^{-1/2}$$

For a better description we need King-models*.
For these introduce tidal radius $R_{\rm t}$, then

$$\langle V^2 \rangle^{1/2} \propto \rho_\circ M(R_{\rm t}) f\left(\frac{R_{\rm t}}{r_\circ} \right)$$

with $f(R_{\rm t}/r_\circ)$ some numerical function.

The central surface density is

$$\sigma_\circ = \rho_\circ r_\circ g\left(\frac{R_{\rm t}}{r_\circ} \right)$$

with $g(R_{\rm t}/r_\circ)$ another numerical function.

*King, A.J. 67, 471 (1962)

For ellipticals $\log(R_t/r_\circ) \approx 2.2$.

With Fish's law (constant central surface brightness) and constant M/L then follows the Faber-Jackson relation* between luminosity L and stellar velocity dispersion σ:

$$L \propto \sigma^4$$

There is also a relation between diameter D_Σ (the radius at which the mean surface brightness is 20.75 mag arcsec^{-2}) and the velocity dispersion†:

$$D_\Sigma \propto \sigma^{4/3}.$$

This can be used to decrease the scatter in the FJ-relation by including surface brightness ($\langle SB_e \rangle$ = mean surface brightness within the effective radius) as a second parameter

$$L \propto \sigma^{2.65} \langle SB_e \rangle^{-0.65}.$$

*Faber & Jackson, Ap.J. 204, 668 (1976)

†Dressler *et al.*, Ap.J. 313, 42 (1987)

The "fundamental plane" of elliptical galaxies is a relation between some consistently defined radius (e.g. core radius) R, the observed central velocity dispersion σ and a consistently defined surface brightness I*:

$$R \propto \sigma^{1.4\pm0.15} I^{-0.9\pm0.1}$$

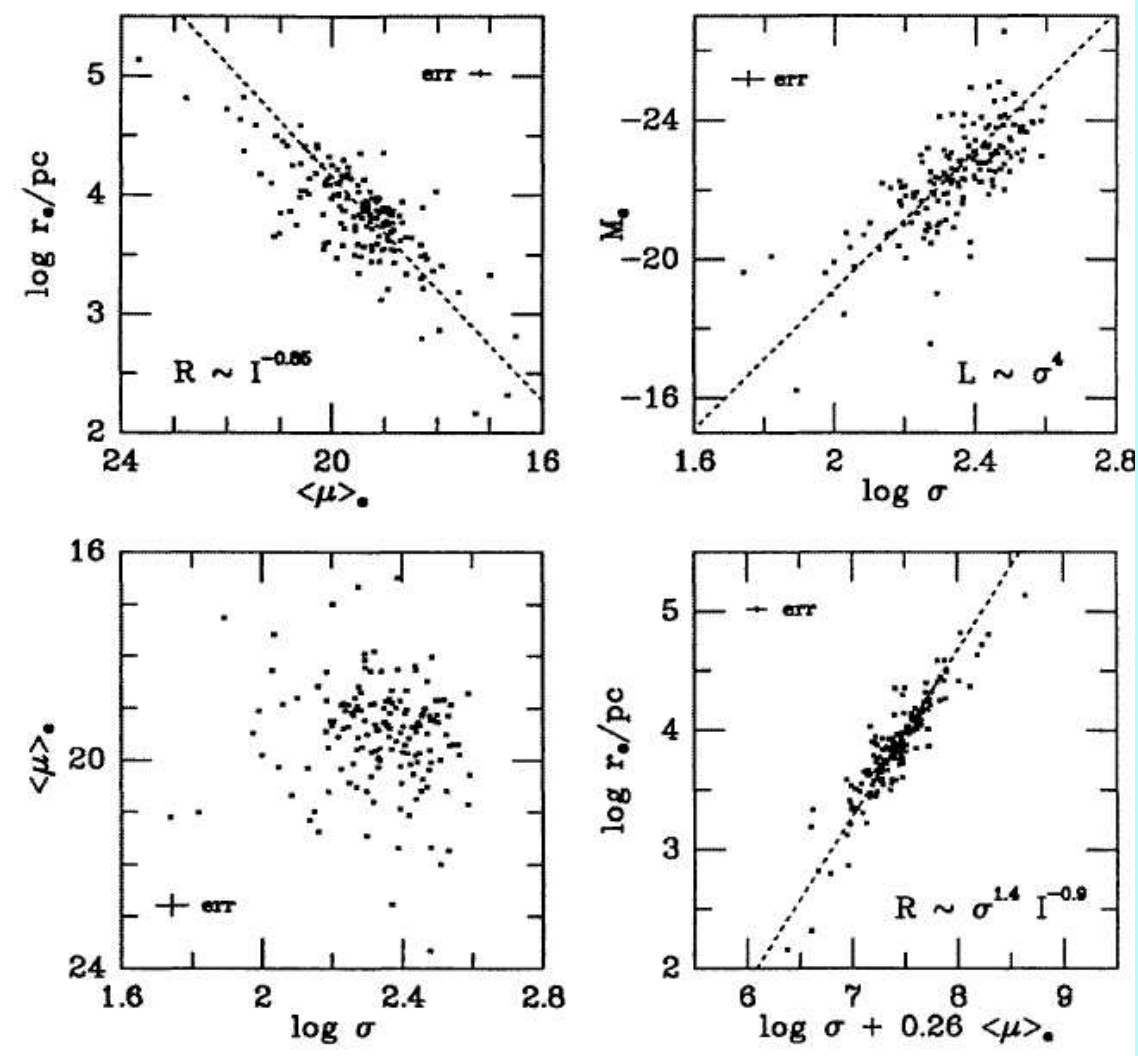

*see Kormendy & Djorgovski, Ann.Rev.Astron.Astrophys. 27, 235 (1989)

In broad terms the Fundamental Plane can be understood as follows.

For equilibrium the Virial Theorem states that

$$2T_{\mathrm{k}} + \Omega = 0$$

where T_{k} is the total kinetic energy and Ω the potential energy.

The kinetic energy is proportional to MV^2 and the potential energy to M^2/R. Here M is the total mass, V a typical internal velocity and R some characteristic radius.

All the information on the detailed density and velocity structure is in the proportionality constants.

Thus we have*

$$M \propto RV^2$$

*For a disk we take the scalelength h for R and de rotation velocity V_{rot} for V. It then easily follows that $M \propto \sigma_{\circ}^{-1} V_{\mathrm{rot}}^4$, which is the Tully-Fisher relation.

For elliptical galaxies the kinetic energy is dominated by that in random motions rather then rotation. So for V we will take the mean velocity dispersion σ.

With the mass-to-light ratio M/L, we replace M with $L(M/L)$ with L the total luminosity.

R remains a typical radius such as the effective radius; then we get

$$R \propto L\frac{M}{L}\sigma^2$$

If I is the mean surface brightness within R we have $I \propto LR^{-2}$ and

$$R \propto \sigma^2 I^{-1}\left(\frac{M}{L}\right)^{-1}$$

The coefficients are close to the observed ones. Differences arise because of variations in actual structural parameters and possible dependence of M/L on M and/or σ.

c. Rotation and shapes.

Originally elliptical galaxies were thought to be simple systems, mainly supported by random motions and flattened by rotation.

The rotation turned out to be too small to provide the flattening so this had to be due to anisotropic velocity distributions.

A parameter used is the ratio of the maximum rotation velocity $V_{\rm m}$ and the observed line-of-sight velocity dispersion at the center $\bar{\sigma}$.

This is a measure of the relative importance of rotation and random motions.

It can be compared to the observed flattening $\epsilon = 1 - b/a$ with a and b the (projected) major and minor axis*.

*Illingworth, Ap.J. 218, L43 (1977)

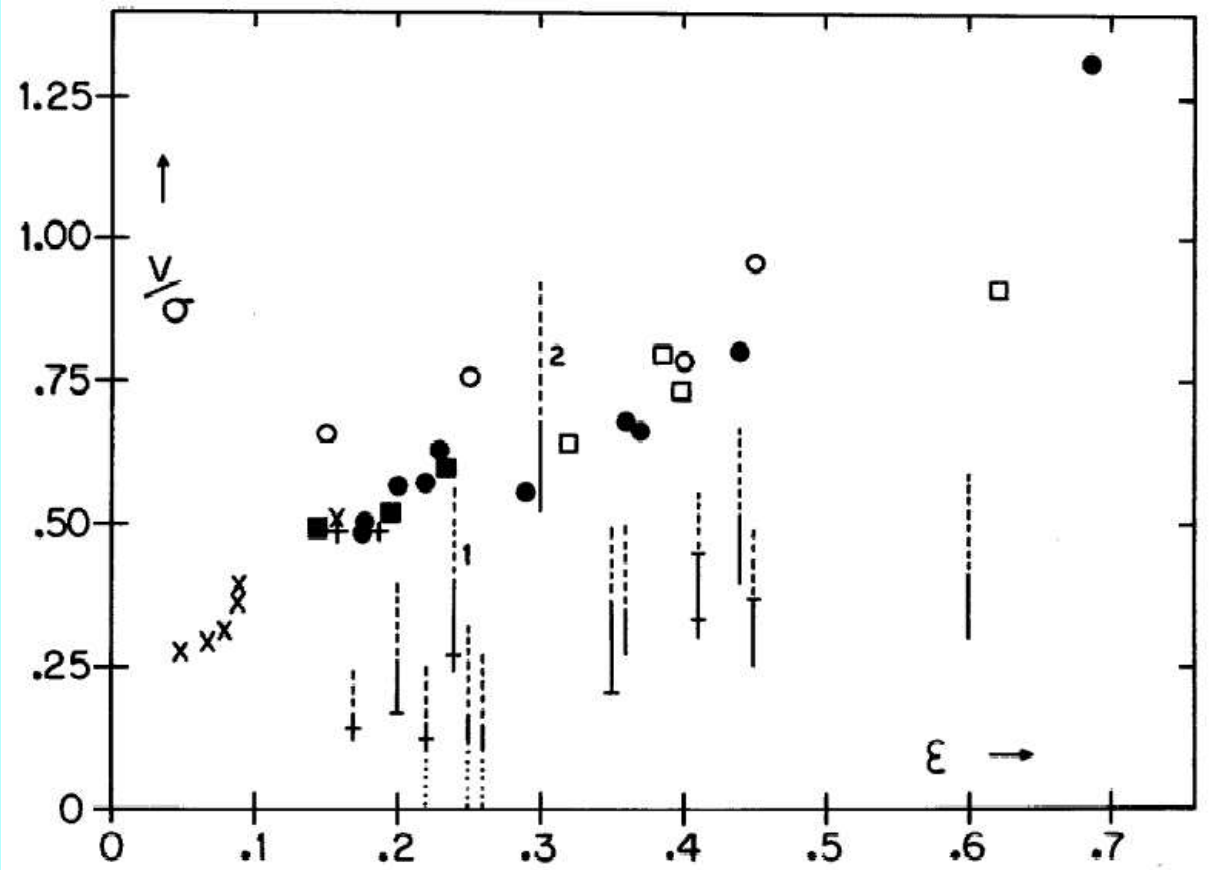

The symbols here indicate models with isotropic velocity dispersions that are flattened by rotation and seen under various inclinations. The bars are data and rotate less than expected for the observed flattening.

Note that the models lie on a well-defined line where the intrinsic relation roughly coincides with the projected one.

Further work* showed that spiral bulges and faint ellipticals are fast rotators.

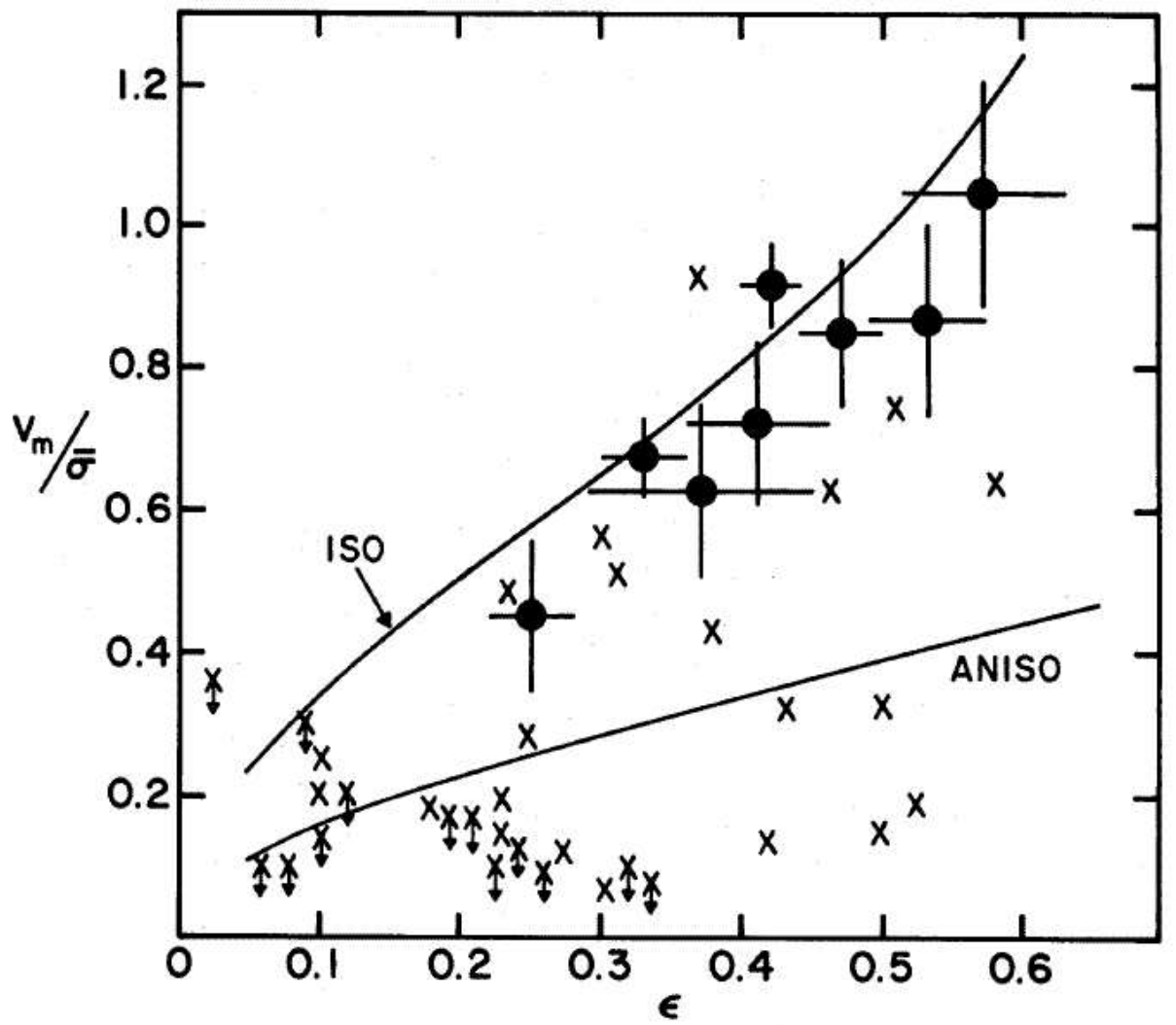

FIG. 3.—Comparison of bulge data (*filled circles*) with all available elliptical galaxy data (*crosses*, *arrows* indicate upper limits) in the dimensionless rotation-ellipticity plane. Derivation of V_m, $\bar{\sigma}$, and ϵ is discussed in the text. The line labeled ISO represents projected models of oblate spheroids with isotropic residual velocities and rotational flattening. The line labeled ANISO describes a typical anisotropic oblate model with σ_z smaller than σ_r and σ_θ.

*e.g. Kormendy & Illingworth, Ap.J. 256, 460 (1982)

Minor axis rotation was first discovered in NGC 4261*.

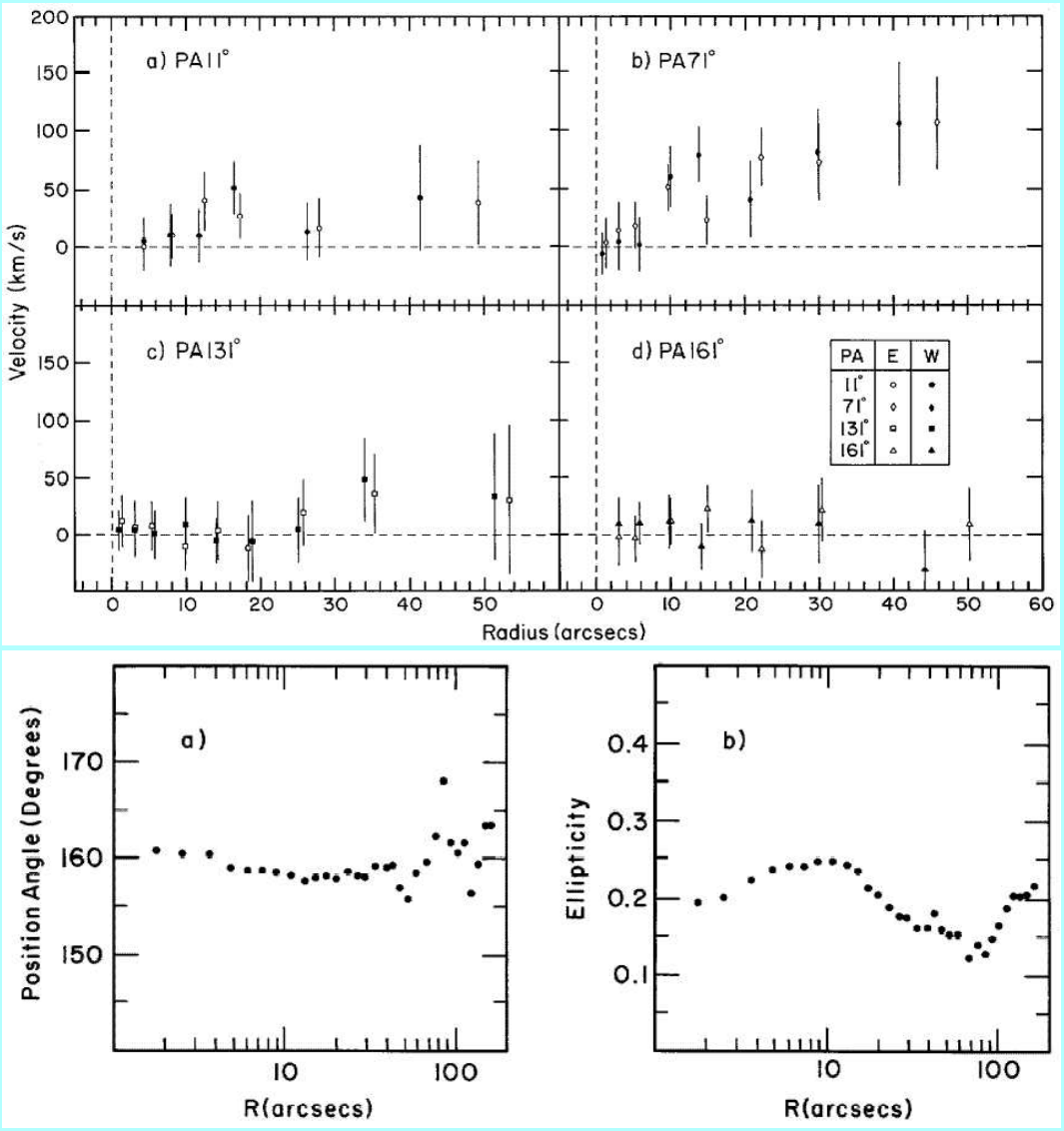

The maximum rotation is in p.a. $\sim 70°$, while the isophotes have major axis at $\sim 160°$.

The suggestion was made that this galaxy is prolate.

*Davies & Birkinshaw, Ap.J. 303, L45 (1986)

It turned out that elliptical galaxies are triaxial*.

This explains the $(V/\sigma - \epsilon)$-relation, the isophote twists and the minor axis rotation.

Minor axis rotation can result from†:
- projection effects in triaxial systems or
- misalingment of the angular momentum and the shortest axis.

Define the misalignment $\psi_{\rm int}$ as the angle between the intrinsic short axis and the angular momentum.

Define for axes $a \geq b \geq c$ the triaxiality

$$T = \frac{a^2 - b^2}{a^2 - c^2} = \frac{1 - b^2/a^2}{1 - c^2/a^2}$$

Thus T=0: oblate; T=1: prolate.

*Binney, Mon.Not.R.A.S. 183, 779 (1978)

†Franx, Illingworth & de Zeeuw, Ap.J. 383, 112 (1991)

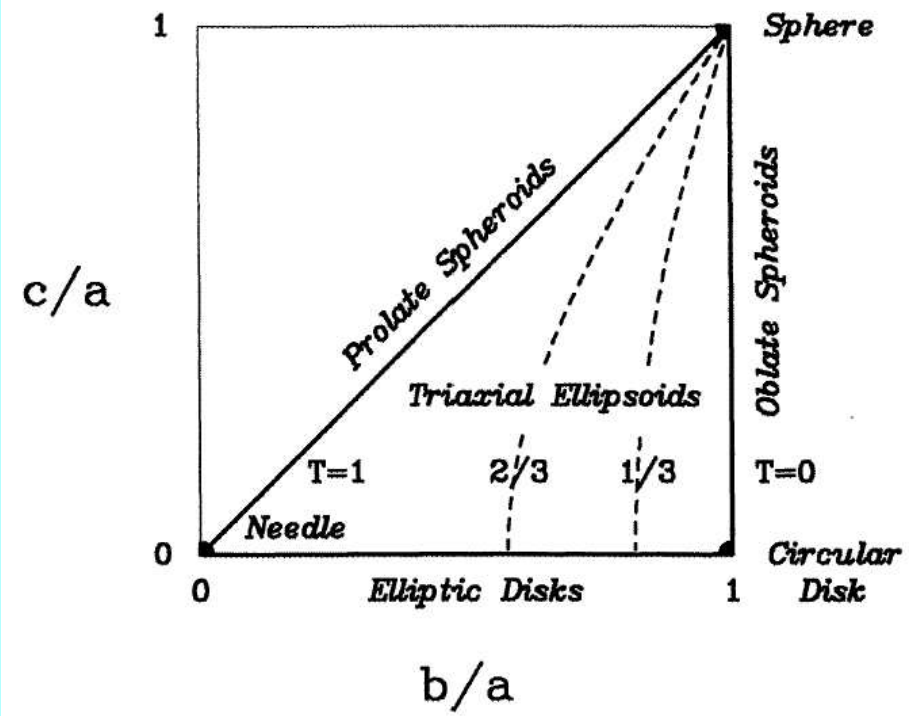

We can *measure* the apparent ellipticity ϵ and the apparent misalignment ψ (the ratio of maximum observed velocity on the apparent axes)

$$\tan\psi = \frac{v_{\rm min}}{v_{\rm maj}}.$$

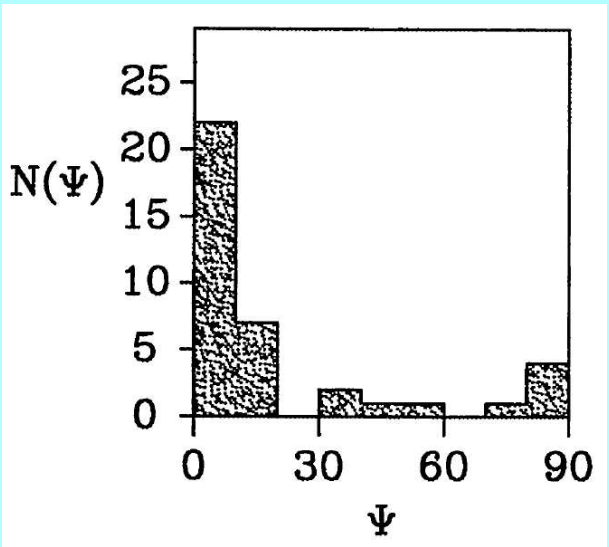

The distributions observed give the following rough indications:

- Most (at least 50%) ellipticals have a small ψ_{int} ($\lesssim 10°$), but some ($\approx 10\%$) rotate along their major axis.
- $\langle T \rangle \approx 0.3$ and T has a wide distribution with possibly as much as 40% of the galaxies prolate.
- The ratio c/a has a peak at about 0.6-0.7.

Dust lanes are often seen* and occur usually along the apparent minor axis, but also sometimes along the major axis.

Here is NGC 1947.

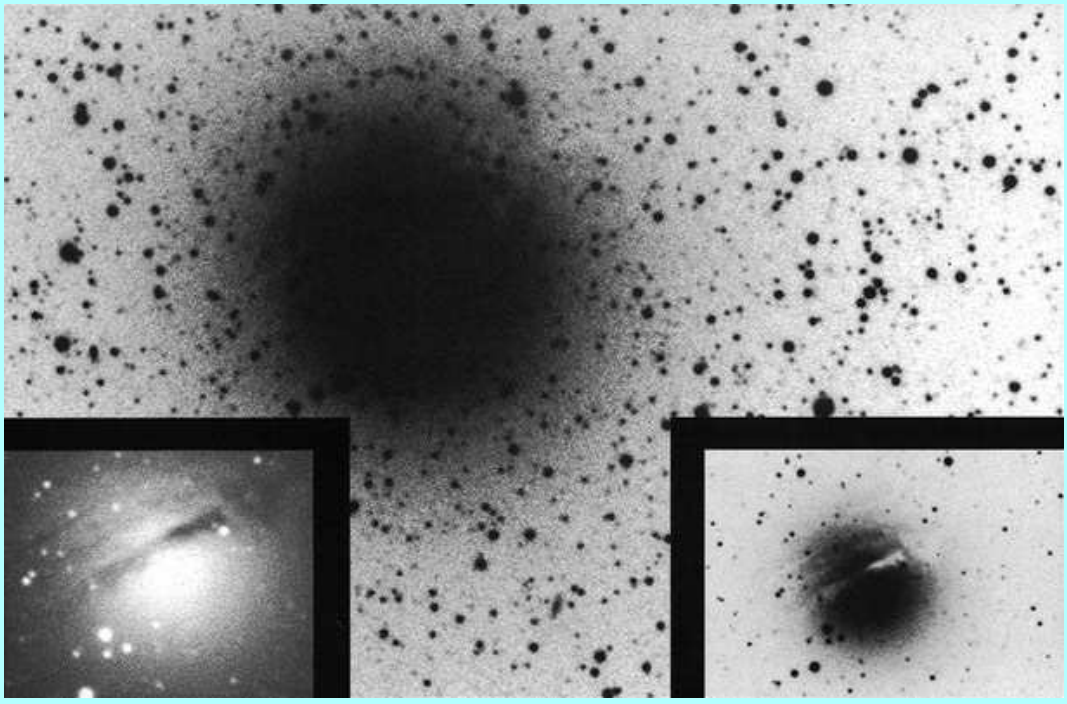

*Bertola & Galletta, Ap.J. 226, L115 (1978)

In triaxial potentials stable orbits are possible, but the detailed kinematics depends on the galaxy shape and body rotation.

In principle dustlanes can be used to determine the intrinsic shape of an individual galaxy *.

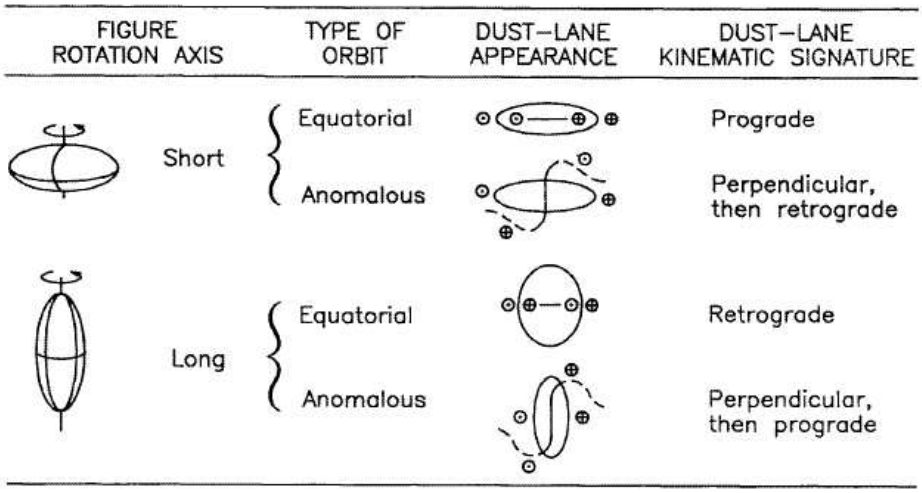

Figure 1 Stable orbits of gas in a rotating triaxial galaxy (adapted from Merritt & de Zeeuw 1983). As illustrated, the figure tumbles in the direction of stellar rotation ($\Omega_p > 0$); if $\Omega_p < 0$, the sense of gas rotation is reversed. Assume that the figure rotates about its shortest or longest axis (*left*). The second column gives the kind of orbit, and the third sketches resulting dust lanes seen edge-on. Anomalous orbits have different orientations at different radii (van Albada et al. 1982). They are the analogues of polar orbits in a stationary potential; at small radii, where Ω_p is unimportant, they are polar. At large radii, the figure rotates several times during an orbit and so is effectively oblate-spheroidal; then the orbit is equatorial (Simonson 1982). In between, the orbits have skew orientations determined by the Coriolis force. The schematic illustrations of dust lanes show the directions of stellar and gas motion; $\odot$ indicates approach, and $\oplus$ indicates recession. The right column states the kinematic signature, i.e. the sense of rotation of the dust lane with respect to the stars.

*Merritt & de Zeeuw, Ap.J. 267, L19 (1983); Kormendy & Djorkovski, Ann.Rev.A&A. 27, 235 (1989)

Detailed kinematics, including higher order moments, of the velocity distributions can now be observed.

An example is a study of NGC3379*.

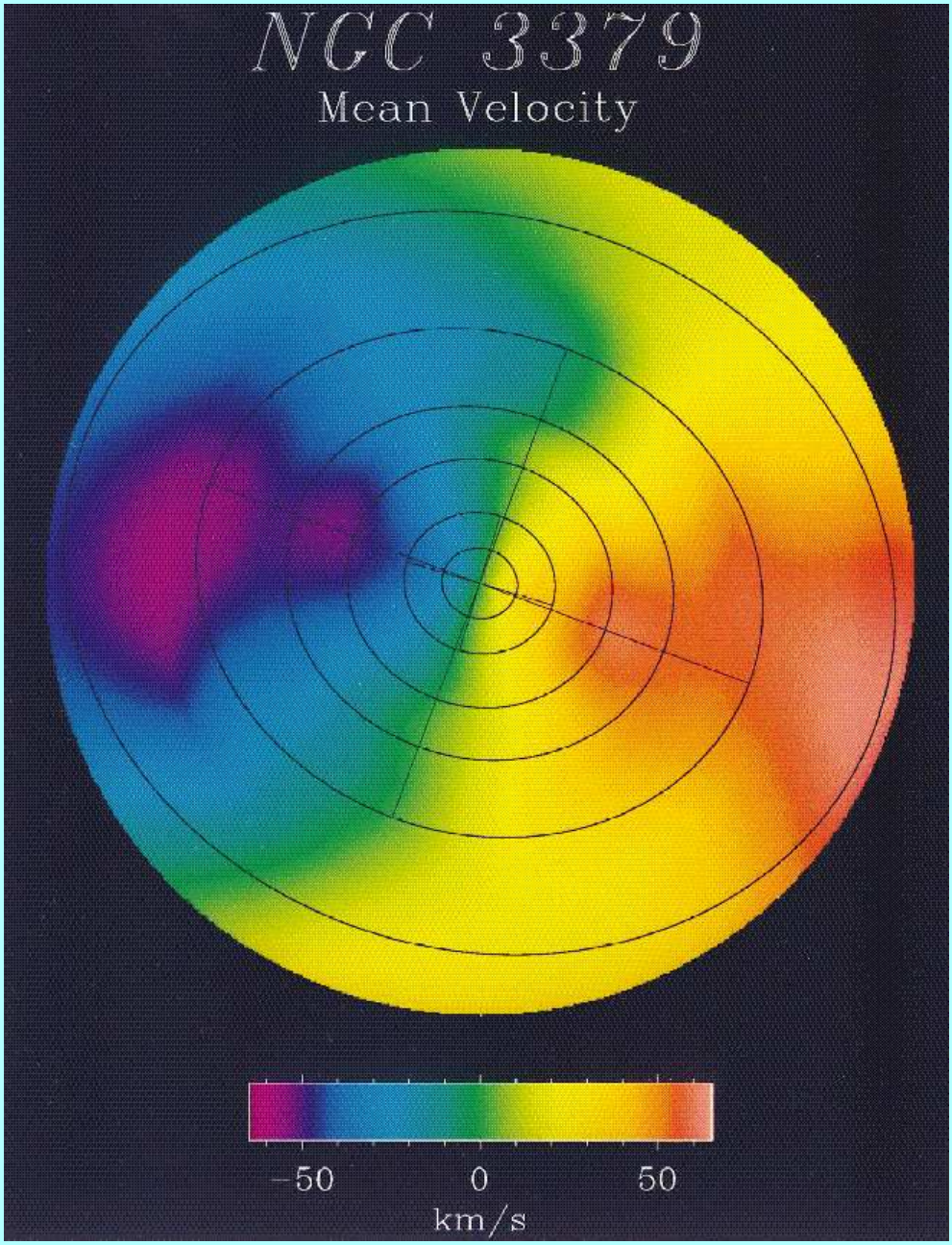

*Statler & Smecker-Hane, A.J. 117, 839 (1999)

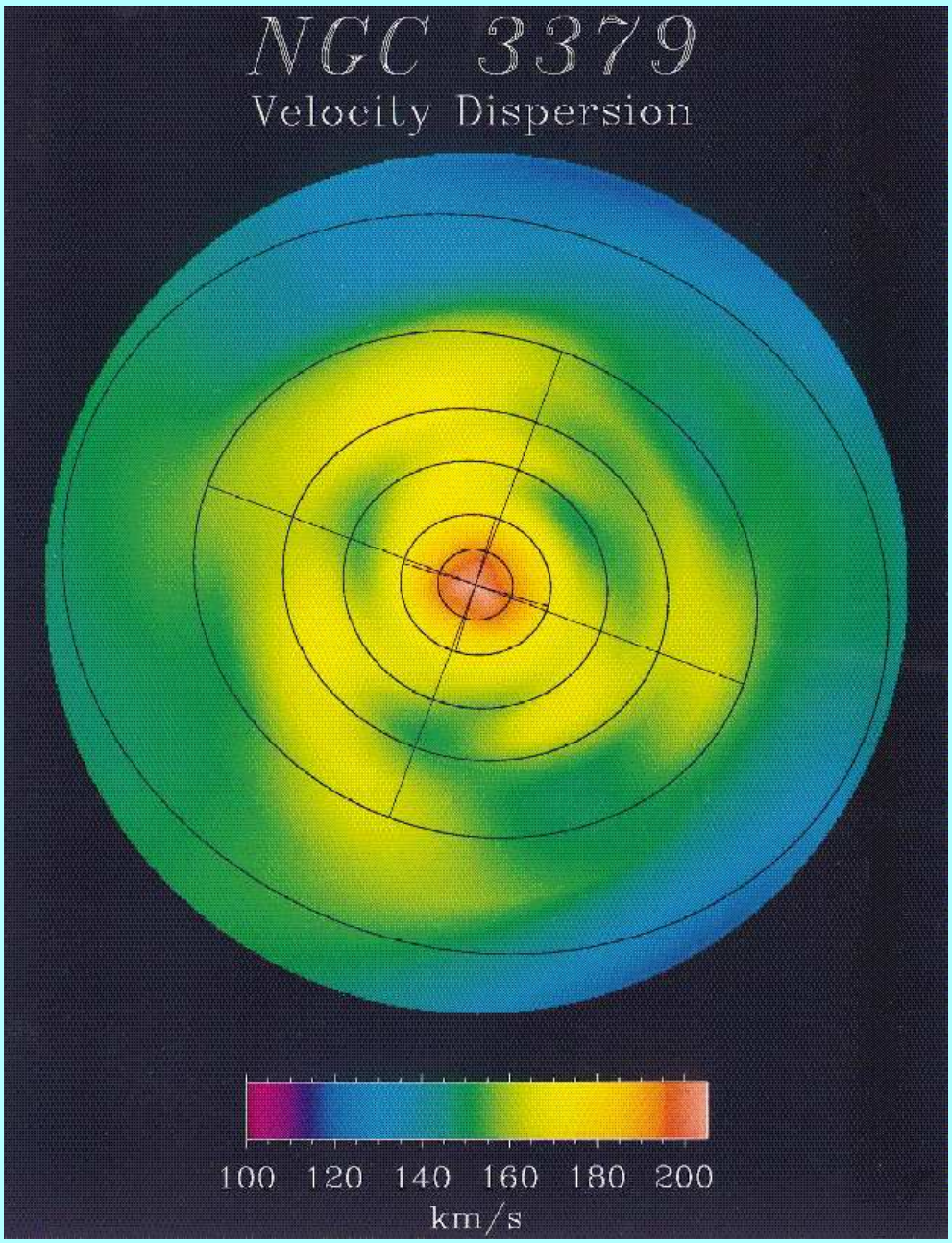
NGC 3379
Velocity Dispersion
100 120 140 160 180 200
km/s

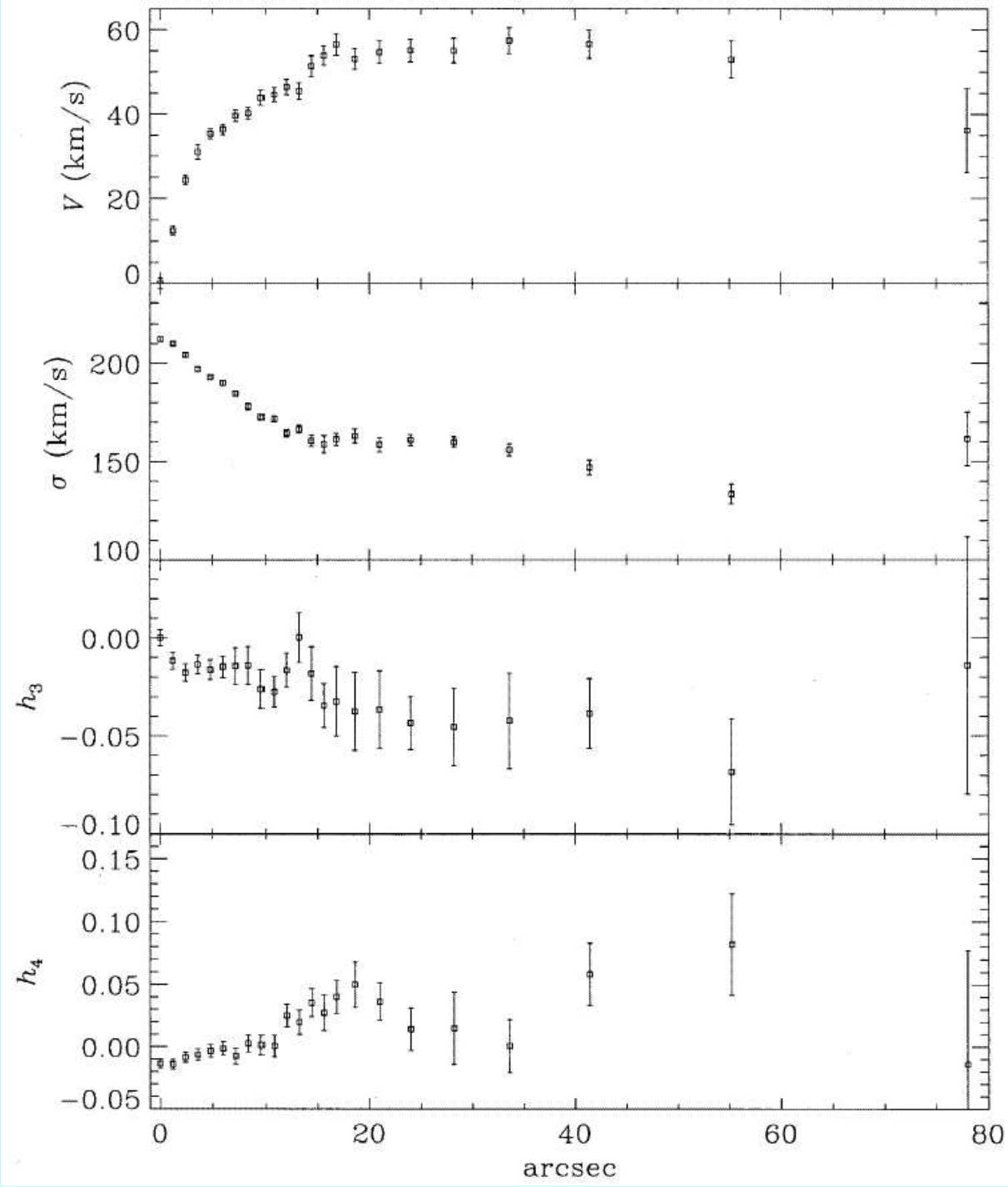

Dynamical modeling shows that NGC 3379 may be a flattened, weakly triaxial system seen in an orientation that makes it appear round.

Recently the SAURON integral field spectrograph has been built and used to survey kinematics and structure of elliptical galaxies*.

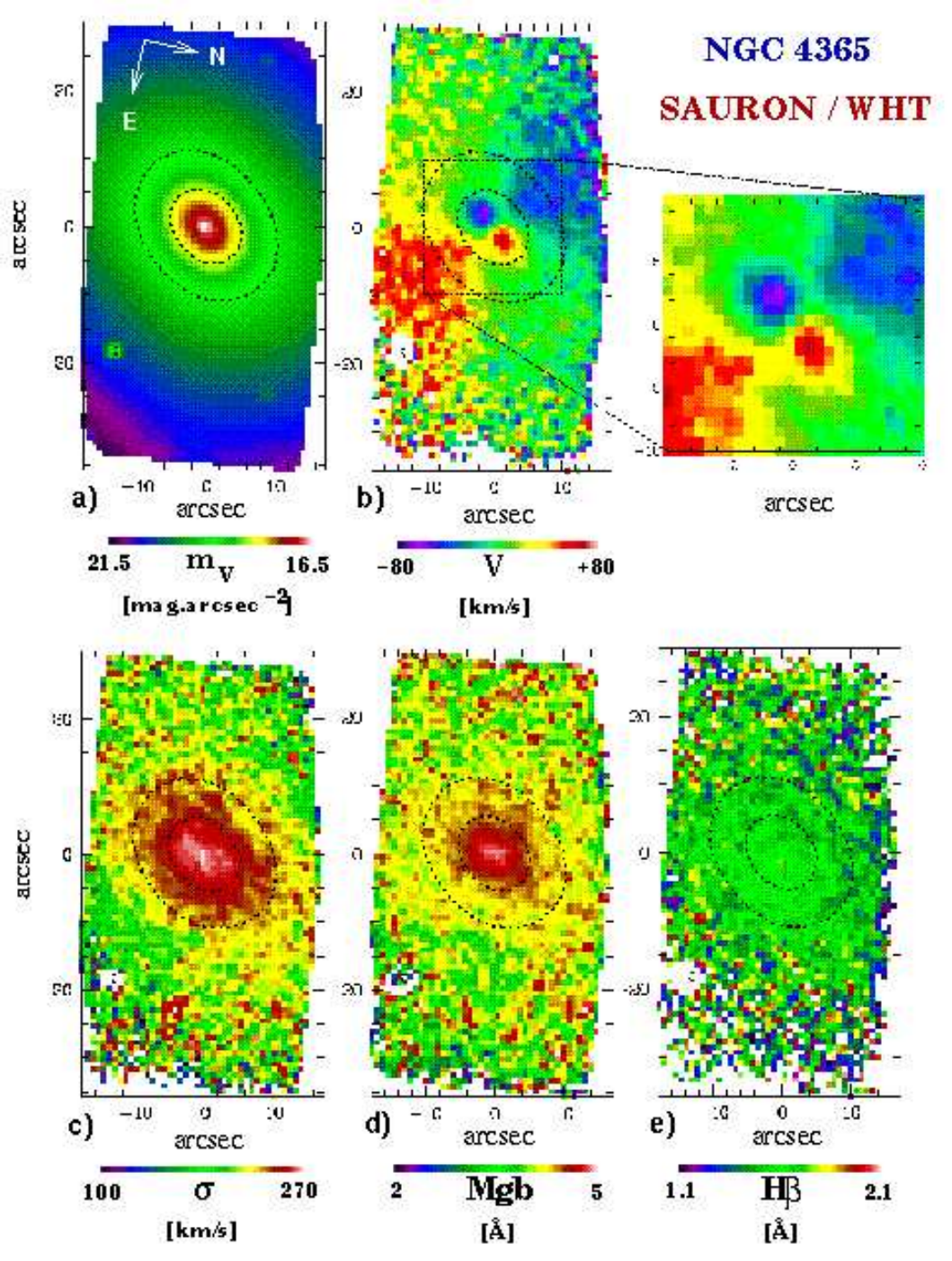

*de Zeeuw et al., Mon.Not.R.A.S. 329, 513 (2002)

d. Central kinematics and black holes.

The central regions often show kinematics deviating from the outer parts.

These distinct cores may show:

- Rapid rotation in the core but slow rotation in the main body
- Opposite rotation in the core relative to that in the main body
- Core rotation along the minor axis.

The distinct cores usually show small velocity dispersions, which suggest a two-component galaxy consisting of an elliptical with a small central disk.

Evidence for black holes comes from rapid rotation and high velocity dispersions in the inner regions, such as in NGC 4594* or our own Galaxy.

*Kormendy et al., Ap.J. 473, L91 (1996)

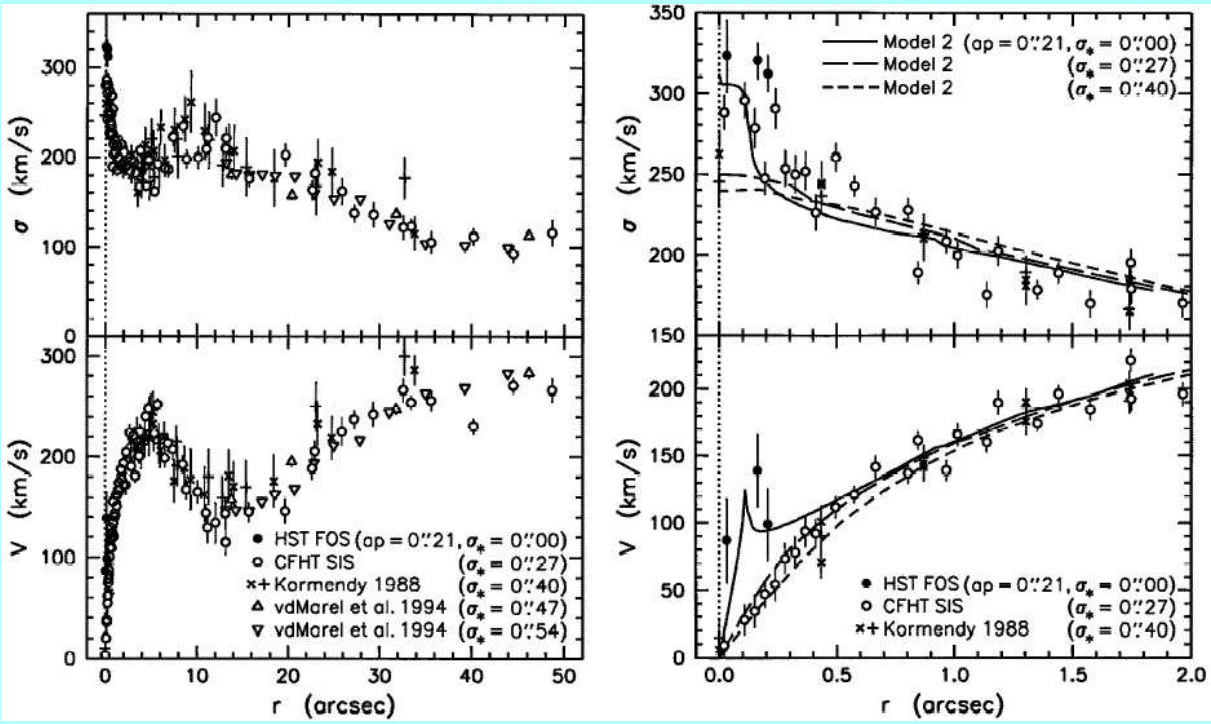
σ (km/s)
v (km/s)
r (arcsec)
HST FOS (ap = 0".21, σ* = 0".00)
CFHT SIS (σ* = 0".27)
Kormendy 1988 (σ* = 0".40)
vdMarel et al. 1994 (σ* = 0".47)
vdMarel et al. 1994 (σ* = 0".54)
Model 2 (ap = 0".21, σ* = 0".00)
Model 2 (σ* = 0".27)
Model 2 (σ* = 0".40)

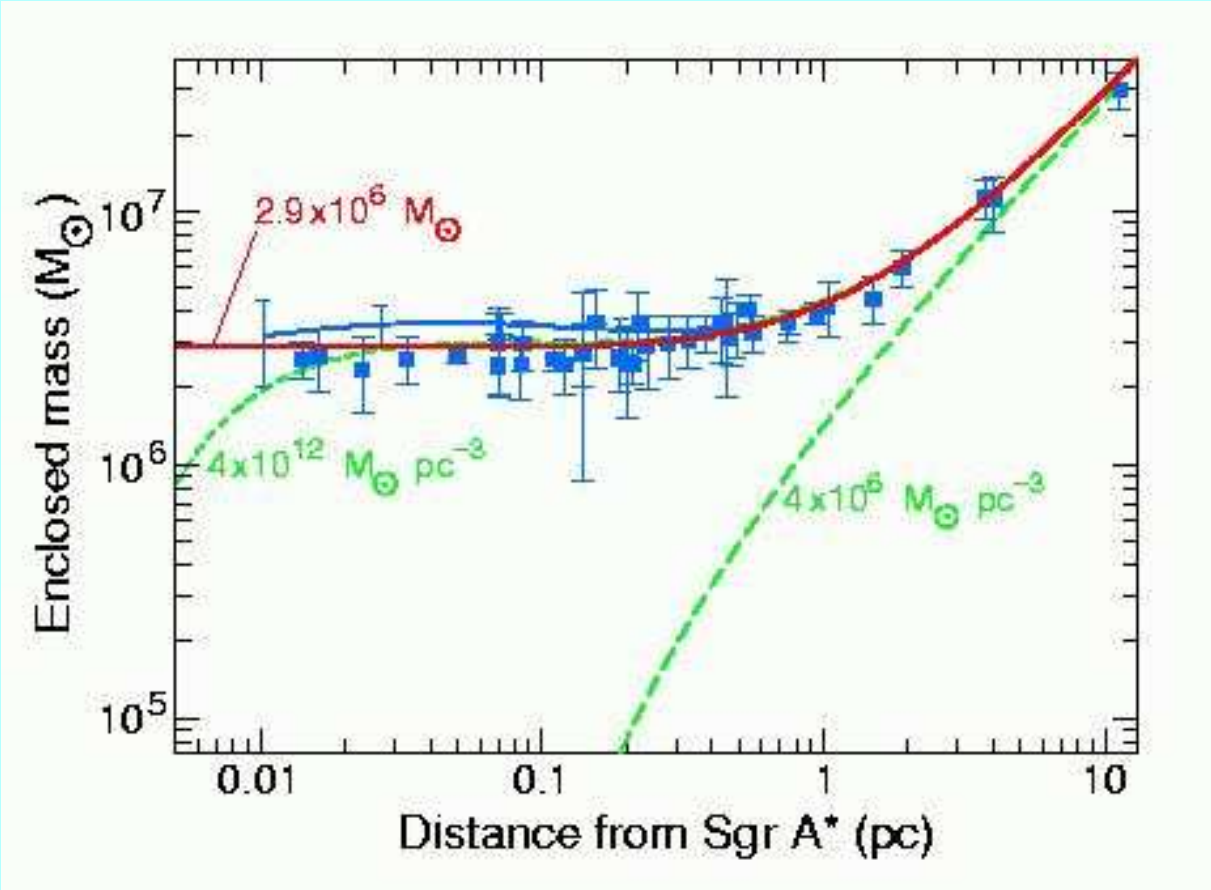
Enclosed mass (M⊙)
Distance from Sgr A* (pc)
2.9x10^6 M⊙
4x10^12 M⊙ pc^-3
4x10^6 M⊙ pc^-3

A compilation of all available data* shows a tight correlation between the mass of the black hole and the luminosity or velocity dispersion in the main body of the elliptical galaxy or bulge.

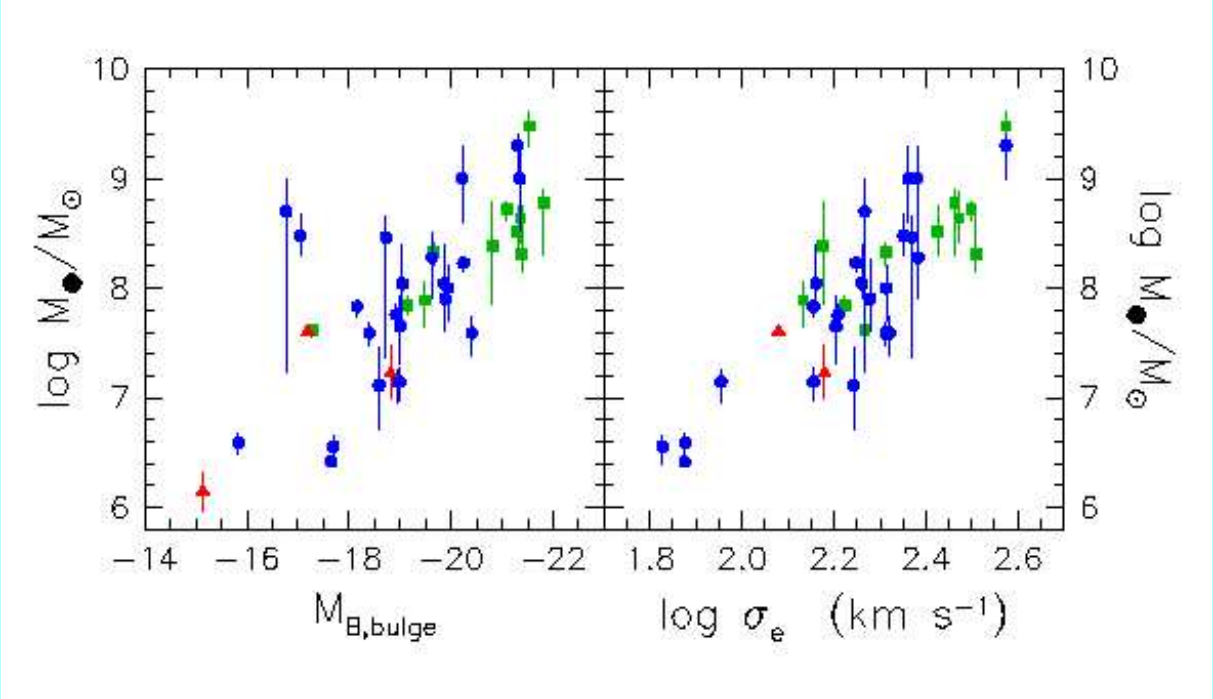

Probably this means no more than that larger galaxies have more material to feed into the center.

*Tremaine et al., Ap.J. 574, 740 (2002)

e. Dynamical models and dark matter.

The most simple description is that of King models, which are isothermal spheres with tidal radii and truncations in the velocity distributions. For these we have can estimate the total mass from

$$\frac{M}{L} = \frac{9\sigma^2}{2\pi G I_0 r_c}.$$

However, we have seen that ellipticals have anisotropic velocity distribrutions and are in general triaxial.

A describtion then is with Stäckel potentials, which are potentials that are separable in ellipsoidal coordinates.

These are coordinates (λ, μ, ν) that are the three roots of τ for

$$\frac{x^2}{\tau + \alpha} + \frac{y^2}{\tau + \beta} + \frac{z^2}{\tau + \gamma} = 1$$

with $\alpha < \beta < \gamma$ three constants.

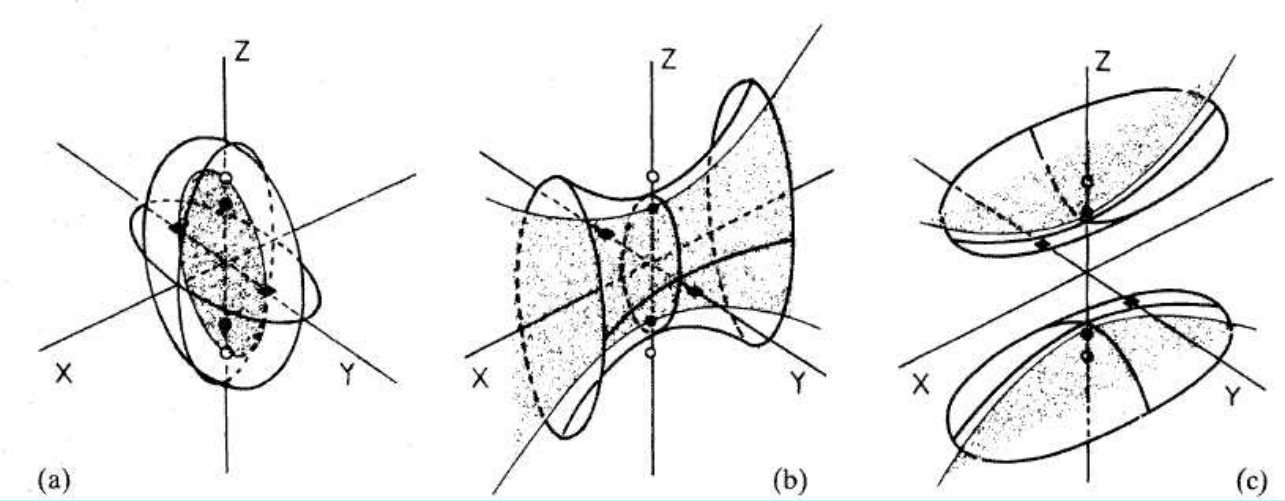

In such coordinate systems surfaces of constant λ are ellipsoids, of constant μ hyperboloids of one sheet and of constant ν hyperboloids of two sheets.

Stäckel potentials are of the form

$$\Phi(\lambda,\mu,\nu) = -\frac{F(\lambda)}{(\lambda-\mu)(\lambda-\nu)} - \frac{F(\mu)}{(\mu-\nu)(\mu-\lambda)} - \frac{F(\nu)}{(\nu-\lambda)(\nu-\mu)}$$

These can be used to describe triaxial galaxies*.

Solutions for isotropic models usually have gradients in M/L, while for triaxial models solutions with constant M/L are usually possible.

*de Zeeuw, Mon.Not.R.A.S. 216, 273 (1985)

X-ray halos at large radii can also be used to measure masses of large ellipticals and clusters.

Measure the emissivity distribution $\epsilon(r)$ from the distribution on the sky and the temperature $T(r)$ from the energy distribution.

Infer from the distribution of ϵ the density distribution of the gas $\rho_{\rm gas}(R)$.

Then the hydrostatic equation gives for the pressure P

$$\frac{dP}{dR} = -\frac{GM(<R)}{R^2}\rho_{\rm gas}(R)$$

The ideal gas equation gives

$$P = \rho_{\rm gas}\frac{kT}{\mu m_{\rm p}}$$

Then

$$M(<R) = -\frac{kT(R)R}{G\mu m_{\rm p}}\left[\frac{d\log\rho_{\rm gas}}{d\log R} + \frac{d\log T}{d\log R}\right].$$

Here are X-ray distributions in two clusters of galaxies.

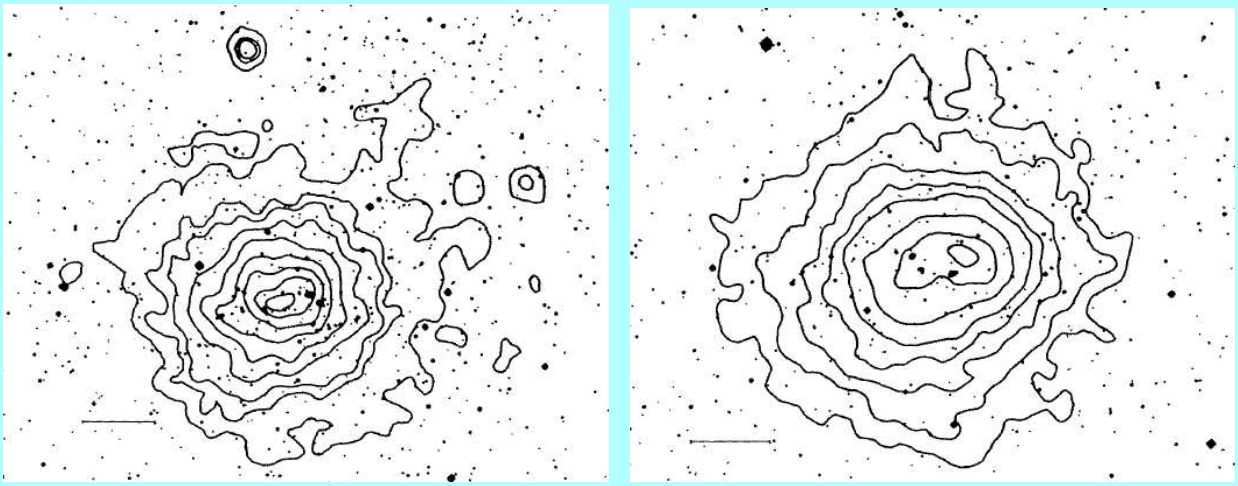

The next two graphs show the analysis of the giant elliptical M 87 in the center of the Virgo cluster*.

*Fabricant & Gorenstein, Ap.J. 267, 535 (1983)

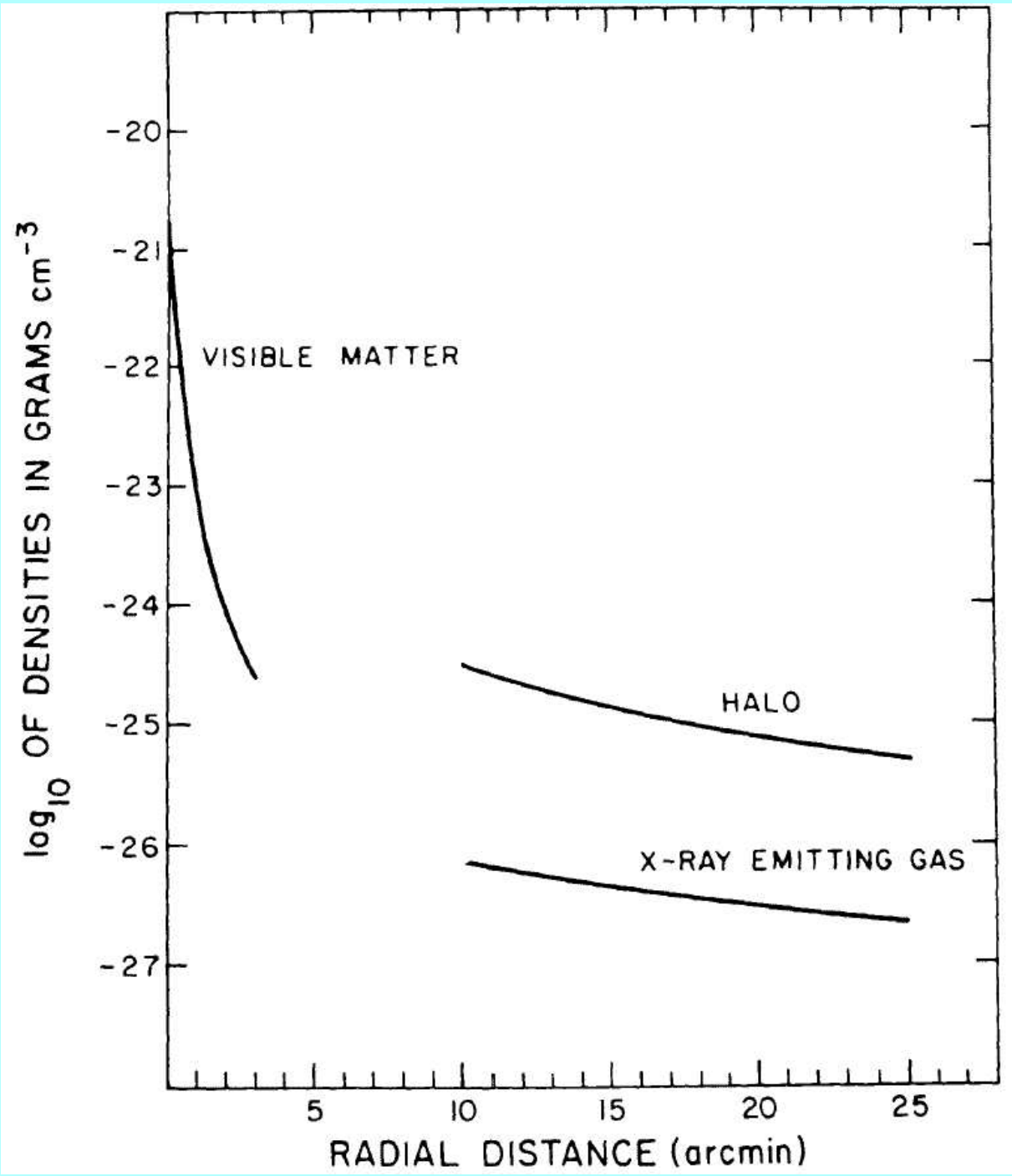
-20
-21
-22
-23
-24
-25
-26
-27
log10 OF DENSITIES IN GRAMS cm-3
VISIBLE MATTER
HALO
X-RAY EMITTING GAS
5
10
15
20
25
RADIAL DISTANCE (arcmin)

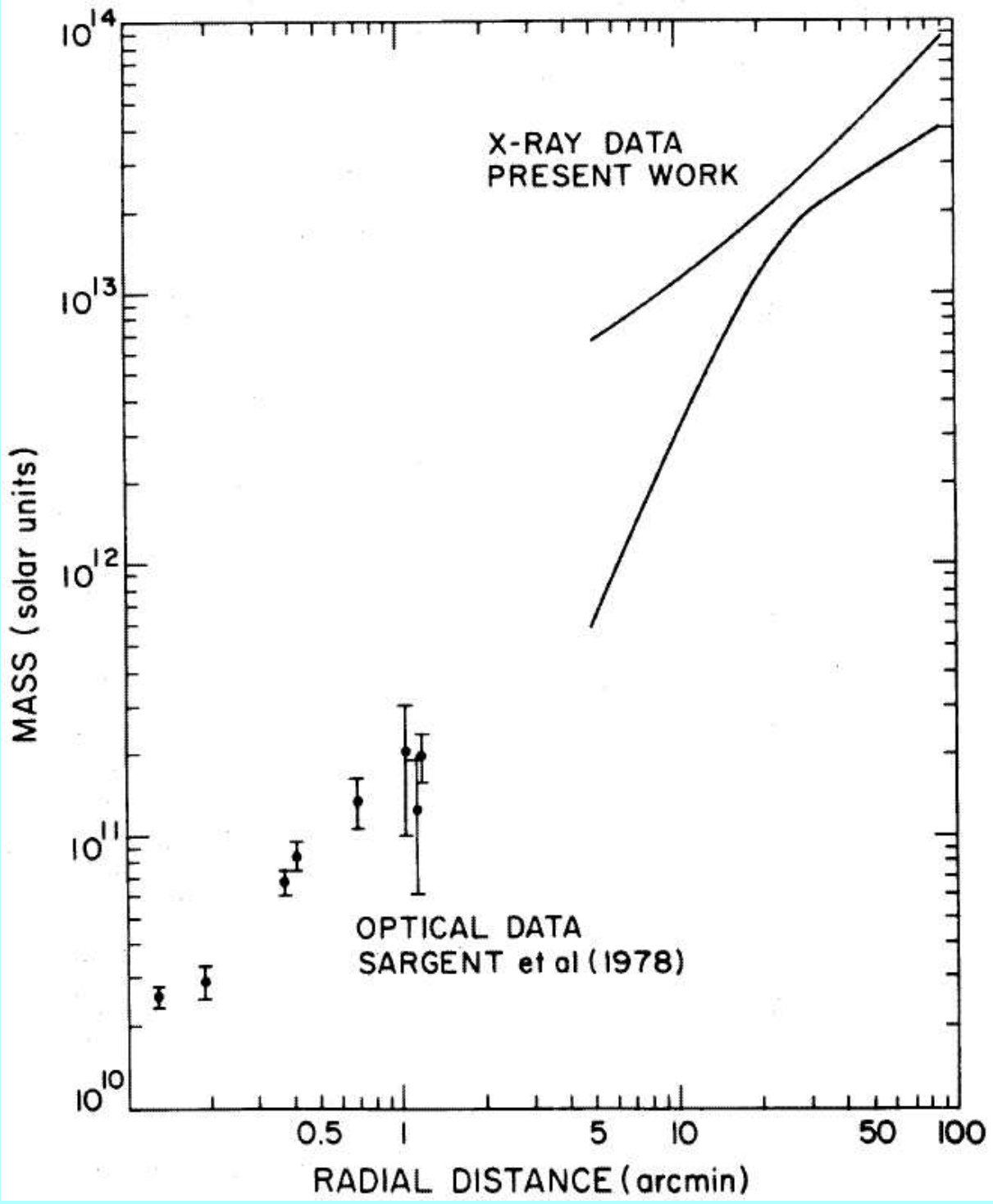
X-RAY DATA
PRESENT WORK
OPTICAL DATA
SARGENT et al (1978)
MASS (solar units)
RADIAL DISTANCE (arcmin)
10^{14}
10^{13}
10^{12}
10^{11}
10^{10}
0.5
1
5
10
50
100

Shells can also be used. Simulations show that their spacing depends on the mass profile.

Finally we can measure masses of whole clusters of galaxies.

The Virial Theorem $2T + \Omega \sim 0$ for equilibrium for a uniform, spherical distribution gives

$$2T = \sum mV^2 \sim M\langle V^2 \rangle \sim -\Omega \sim \frac{3GM}{5R}$$

Thus

$$M \sim \frac{R\sigma_{\mathrm{v}}^2}{G} \sim \left(\frac{R}{1\ \mathrm{Mpc}}\right)\left(\frac{\sigma_{\mathrm{v}}}{10^3\ \mathrm{km\ s^{-1}}}\right)^2 10^{15}\ \mathrm{M}_\odot$$

This indicates masses of up to $10^{15}\ \mathrm{M}_\odot$.

Nowadays also gravitational arcs can be used*.

*e.g. in Abell 2218 by Kneib et al., A.&A. 303, 27 (1995)

Gravitational Lens in Abell 2218 HST · WFPC2

PF95-14 · ST ScI OPO · April 5, 1995 · W. Couch (UNSW), NASA

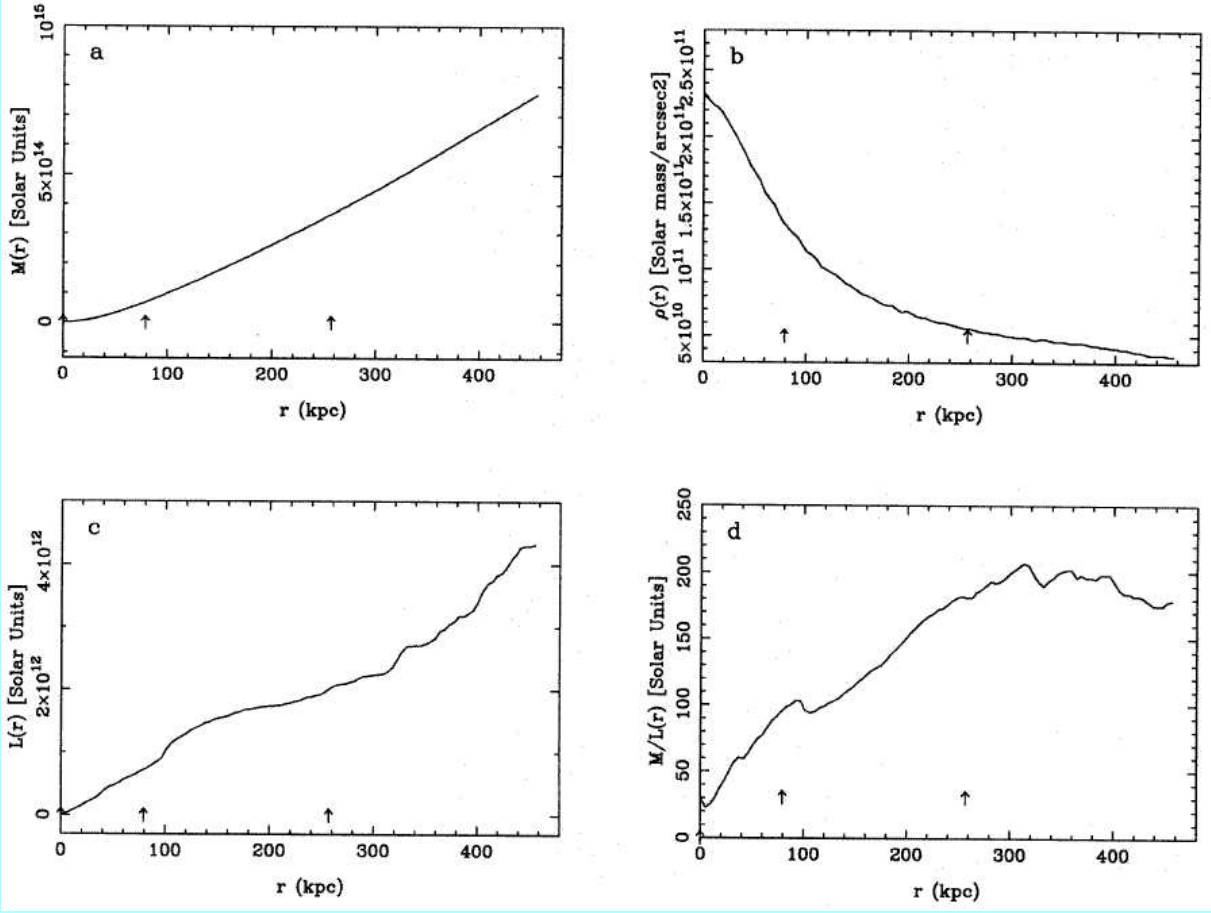

f. Color gradients.

Important for formation models is the correlation of color gradients with structural and dynamical properties.

Color gradients usually are defined as the change in color index in magnitudes per decade in radius or $\bigtriangledown(B-V) = \Delta(B-V)/\Delta(\log r)$.

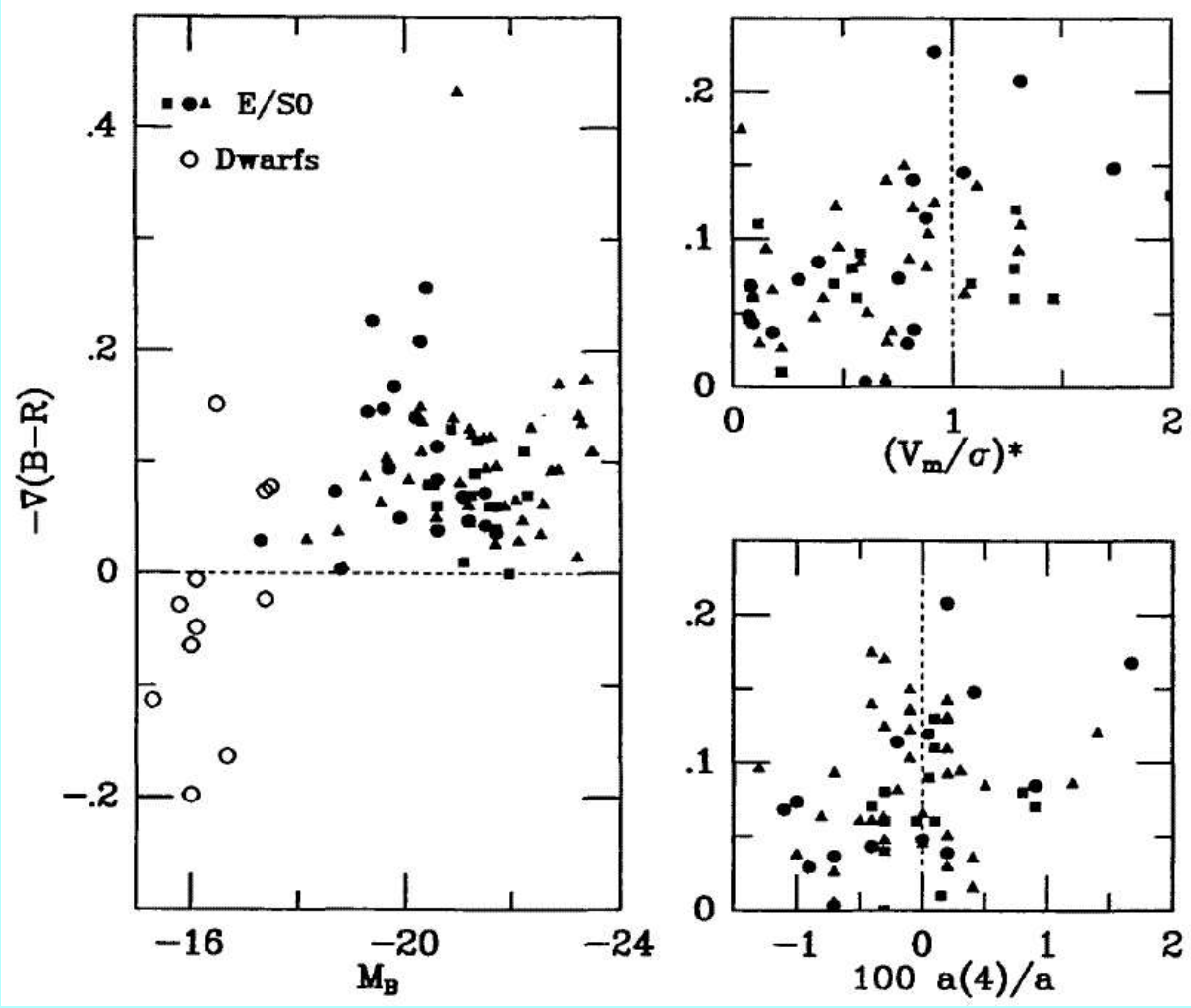

The property $(V_m/\sigma)^*$ is normalised to unity for an isotropic oblate rotator.

- Ellipticals have significant color gradients. The light becomes redder towards the center.

- However, dwarf spheroidals have inverse gradients. This may be due to recent star formation.

- Anisotropic galaxies have smaller gradients.

- Also boxy galaxies tend to have smaller gradients.

- There is no strong correlation between the strength of the color gradient and the luminosity or velocity dispersion.

g. Formation.

The oldest idea is that elliptical galaxies form through a dissipative process, where a relatively slowly contracting gas cloud forms stars and is slowly being enriched*.

This was thought to be the only way of getting color and metallicity gradients.

However, color gradients should correlate with luminosity, if the collapse is dissipative and this is not observed.

Dissipational collapse occurs when very early on a major fraction of the gas is turned into stars.

During the collapse violent relaxation takes place in the rapidly (relative to orbital periods) changing gravitational field.

*Larson, Mon.Not.R.A.S. 166, 585 (1974) and 173, 671 (1975)

Van Albada* was the first to simulate violent relaxation in numerical experiments.

He found that for irregular initial conditions and large collapse factors an $R^{1/4}$-law results for the region containing between 10 and 99% of the mass.

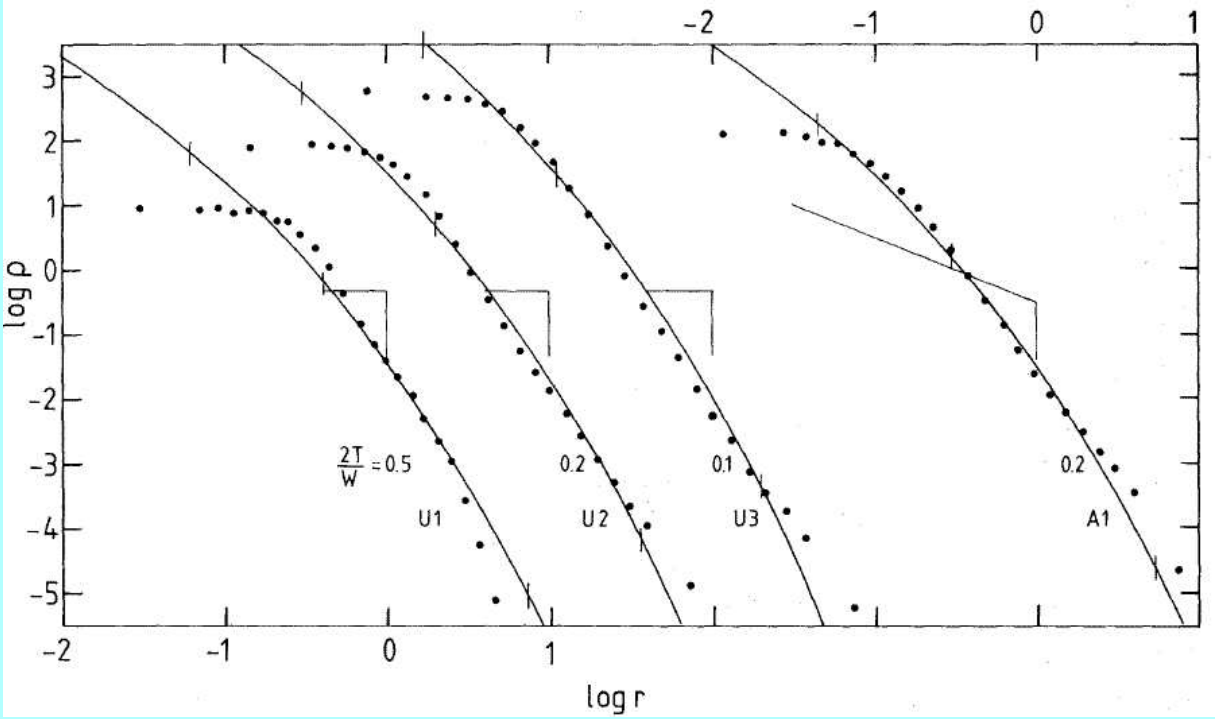

He also found that the total energy of stars before and after collapse was correlated and therefore color and abundance gradients can survive violent relaxation.

*Mon.Not.R.A.S. 210, 939 (1982)

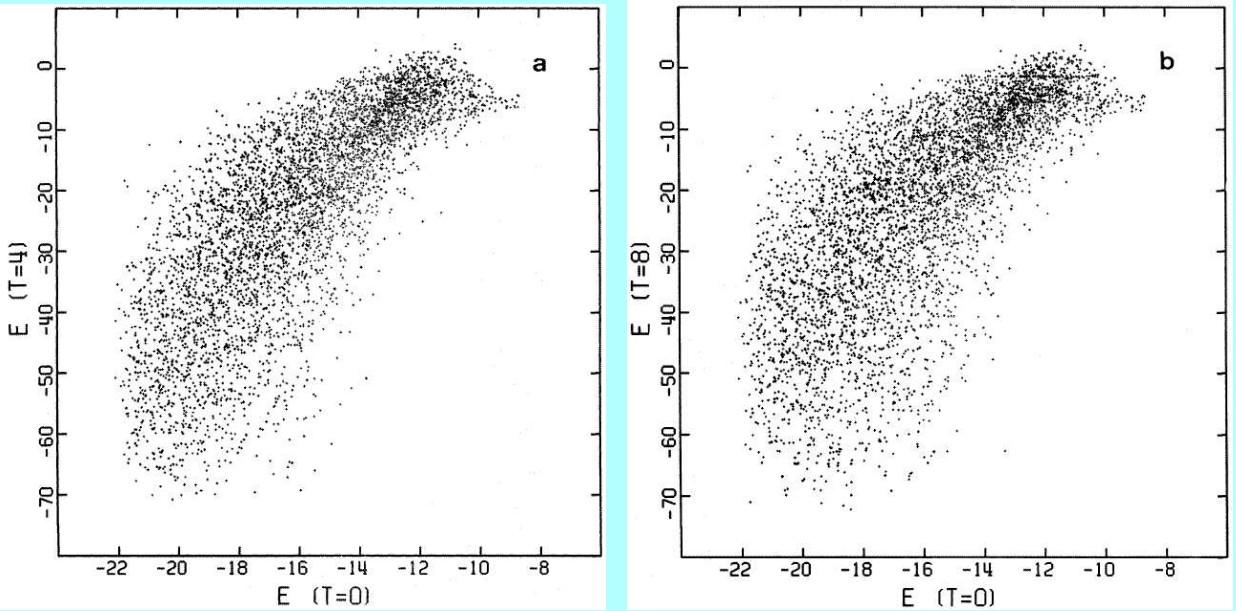

In particular for giant ellipticals and cD's in clusters merging is likely to be important.

The current observed rate of spiral mergers (from interacting galaxies) is high enough to produce the majority of ellipticals.

Merging may be the cause of the following:

- The observed low rotation in bright ellipticals.
- The presence of shells and ripples.
- The occurence of kinematically distinct cores and multiple nuclei.

Studies of clusters with central ellipticals with multiple nuclei* have been done, correcting the brightness distribution for the infalling galaxies.

This shows that a merger rate of up to 2 L* per 5×10^9 years is possible for the brightest cluster galaxies.

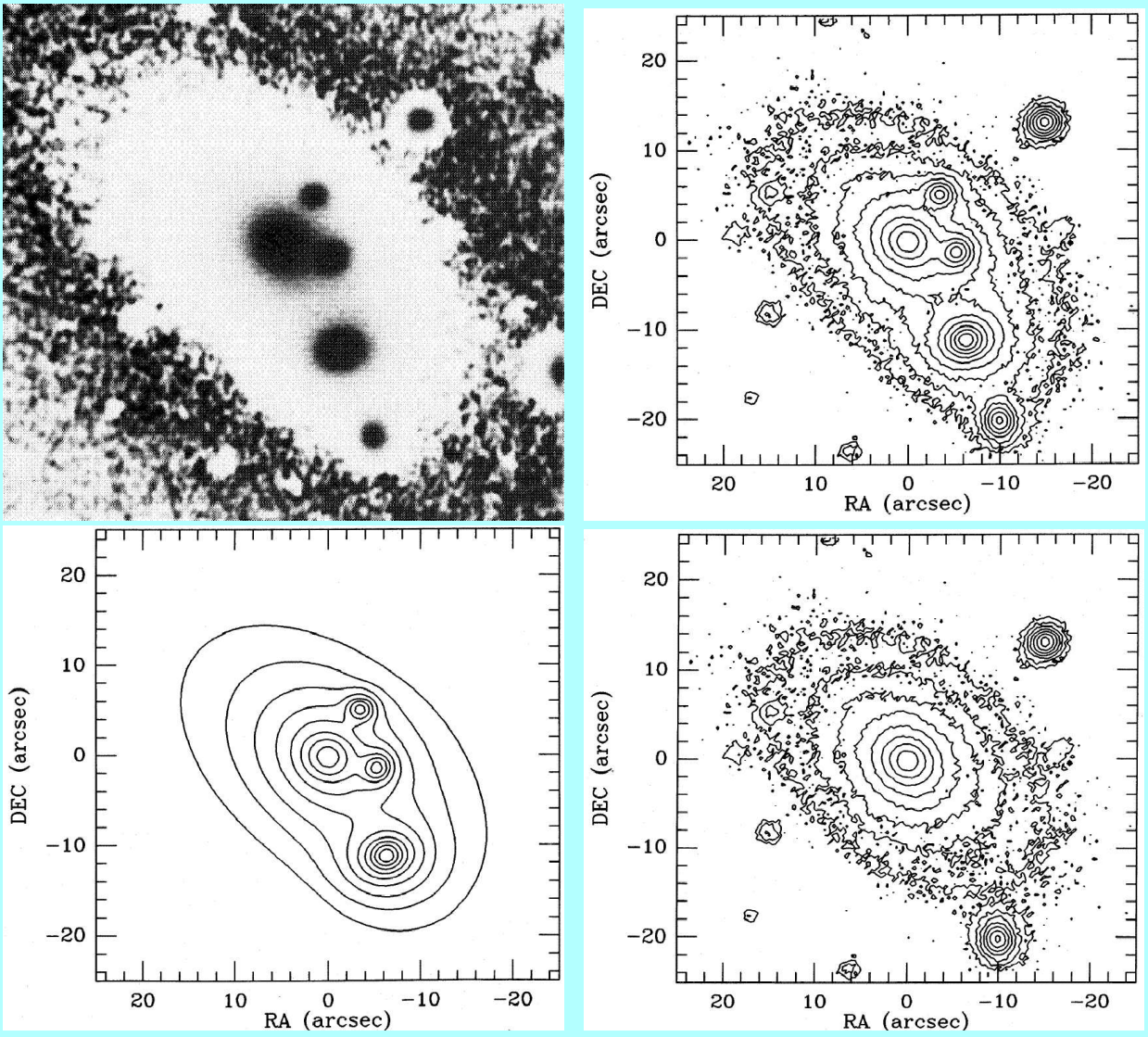

*e.g. Lauer, Ap.J. 325, 49 (1988)